Carbohydrate Polymers 368 (2025) 124070

Contents lists available at ScienceDirect

Carbohydrate Polymers

journal homepage: www.elsevier.com/locate/carbpol

Valorization of metabolite-enriched carbohydrates from *Theobroma* biomass via ultrasound-assisted alkaline extraction

Jose Manuel Núñez-Ramírez [a,1], Andrea Martelli [b,1], Tabitha Halliday [c], Bradley Thomas [d], Corinne Wills [e], Valeria Cannillo [b], Devis Bellucci [b], Carlos Carranza [f], Paola A. García-Rincón [a], Piergiorgio Gentile [g,h,*,2], Joel Girón-Hernández [d,h,*,2]

[a] *Facultad de Ciencias Agropecuarias, Maestría Sistemas Sostenibles de Producción, Universidad de la Amazonia, 180001 Florencia, Colombia*
[b] *Dipartimento di Ingegneria Enzo Ferrari, Università degli Studi di Modena e Reggio Emilia, 41125 Modena, Italy*
[c] *Department of Geography and Environmental Sciences, Northumbria University, NE1 8ST Newcastle Upon Tyne, United Kingdom*
[d] *Department of Applied Sciences, Faculty of Health and Life Sciences, Northumbria University, NE1 8ST Newcastle Upon Tyne, United Kingdom*
[e] *School of Natural and Environmental Sciences, Newcastle University, NE1 7RU Newcastle upon Tyne, United Kingdom*
[f] *Escuela de Ciencias Agrícolas, Pecuarias y del Medio Ambiente, Universidad Nacional Abierta y a Distancia, 111511 Bogotá, Colombia*
[g] *School of Engineering, Newcastle University, NE1 7RU Newcastle Upon Tyne, United Kingdom*
[h] *Centre for Biomaterials and Tissue Engineering (CBIT), Universitat Politècnica de València, 46022, Valencia, Spain*

ARTICLE INFO

Keywords:
Theobroma biomasses
Biopolymers
Pectin
Alkaline extraction
Ultrasound-assisted extraction
Principal component analysis

ABSTRACT

Polysaccharides, widely used in food, pharmaceutical and industrial sectors, are abundant in *Theobroma* species pod husk waste (*T. cacao*, *T. grandiflorum* and *T. bicolor*). This study examined alkaline extraction using NaOH and KOH with ultrasound assistance to assess the physicochemical and functional properties of the resulting polysaccharides and non-polysaccharides components. The extraction yields of these components varied, with *T. cacao*-NaOH yielding the highest recovery (38.0 %), followed by *T. bicolor*-NaOH (14.7 %) and *T. grandiflorum*-NaOH (8.0 %). NaOH-extracted materials exhibited galacturonic acid content up to 40 %, molecular weight of ~783 kDa and esterification degree of 38.1 %, while KOH-based extraction retained higher levels of rhamnose (18.0 %) and xylose (28.3 %). Materials extracted via KOH preserved metabolites like proanthocyanidins (1.58 mg catechin equivalent/g in *T. grandiflorum*), whereas NaOH extraction resulted in greater antioxidant activity, particularly in *T. cacao* with 127.8 mmol Fe^{2+}/g and 3.26 M Trolox equivalent/g in FRAP and ORAC assays. Rheology showed that polysaccharides extracted from *T. cacao* and *T. bicolor* exhibited highest viscosity and gel strength ($G' > G''$), while those from *T. grandiflorum* had lower viscosity. Thermal analyses confirmed that NaOH extractions produced stable, gel-forming polysaccharides associated with pectic components. These findings highlight *Theobroma* pod husks as a valuable waste source for revalorization.

1. Introduction

The *Theobroma* genus, part of the *Malvaceae* family, includes plants native to tropical America, valued for their bioactive compounds like alkaloids, flavonoids and fats (Benlloch-Tinoco et al., 2024). *Theobroma cacao* is the most recognized species due to its role in chocolate production, but other species, such as *Theobroma. grandiflorum* (cupuaçu) and *Theobroma. bicolor* (macambo), have gained attention for their high-quality fats and unique flavor profiles (Febrianto & Zhu, 2022). Despite these valuable properties, these fruits present a challenge: the considerable waste generated during post-harvest processing. Up to 70 % of *T. cacao* fruit is discarded (Girón-Hernández, Rodríguez, et al., 2024), resulting in a substantial biomass that could be harnessed for its bioactive compounds. In particular, this biomass, including its seeds, pod husks, pulp and leaves, contains a rich diversity of biocompounds and biopolymers that have significant ecological, nutritional and industrial value (Jean-Marie et al., 2022). Among these, polyphenols are particularly prominent, contributing to the antioxidant properties of the

* Corresponding authors at: Center for Biomaterials and Tissue Engineering (CBIT), Universitat Politècnica de València, 46022, Valencia, Spain.
E-mail addresses: pgentil@upvnet.upv.es (P. Gentile), joel.l.g.hernandez@northumbria.ac.uk (J. Girón-Hernández).
[1] These authors contributed equally to this work.
[2] These authors supervised equally this work.

https://doi.org/10.1016/j.carbpol.2025.124070
Received 13 February 2025; Received in revised form 27 June 2025; Accepted 14 July 2025
Available online 15 July 2025

biomass. Flavonoids, such as catechins, epicatechins and proanthocyanidin, are abundant in *Theobroma* seeds and pod husks, offering health benefits and enhancing food stability. Phenolic acids, including gallic and caffeic acids, are also present, contributing to bioactivity and potential therapeutic properties of *Theobroma* biomass (Mar et al., 2024). Another significant class of compounds, methylxanthines, primarily theobromine and caffeine, exhibit stimulatory effects and plant defense roles, with the highest concentrations in seeds but can also be detected in other parts of the plant (Kieck et al., 2016). Furthermore, the biopolymers in the *Theobroma* genus include polysaccharides such as cellulose, hemicelluloses and pectins, essential for plant integrity. These polysaccharides are particularly prominent in the pod husks and play an important role in applications such as biodegradable packaging and bioenergy production (Mar et al., 2024). Revalorizing biomass for biopolymer extraction holds significant importance due to its potential to create sustainable materials, reduce agricultural waste and support bioeconomy initiatives. The comprehensive biochemical composition of *Theobroma* biomass highlights its value across various sectors, including food, cosmetics and pharmaceuticals. This diversity underscores the importance of exploring the full potential of the genus as a source of bioactive compounds and renewable materials.

To address this, researchers have explored various methods to valorize *Theobroma* residual biomass, primarily using acidic solutions (Barrios-Rodríguez et al., 2022); however, these approaches are often limited by extraction yields below 10 % (Jarrín-Chacón et al., 2023; Vriesmann et al., 2012). Recently, enzymatic and alkaline extractions aided by ultrasound (US) have been explored (Girón-Hernández, Rodríguez, et al., 2024). Moreover, alkalization is aligned with existing methods used in the cocoa processing industry to reduce the acidity of the beans and modify flavor, color and solubility by adding alkalis like NaOH, KOH, K_2CO_3 or $NaHCO_3$ to cocoa powder or mass; this process also impacts the material's elastic modulus, a measure of its stiffness, which is crucial for understanding how a material behaves under different forces (Puchol-Miquel et al., 2021). In addition, studies on cocoa paste alkalinization have investigated how different alkaline solutions affect the content of metabolites in the final product. Indeed, phenols in cocoa exist in free or non-extractable forms (bound to other molecules or cellular structures) and these can be released during alkalization with NaOH. One study reported that clovamide was the only polyphenol present at higher concentrations in cocoa compared to commercial varieties following treatment with a NaOH solution and subsequent extrusion (Valverde et al., 2020). Therefore, alkaline extraction effectively breaks down plant matrices by hydrolyzing ester bonds in protopectin, facilitating soluble pectin release. This method is particularly advantageous for extracting gel-forming polysaccharides associated with pectin components, making them suitable in industry (Yang et al., 2024).

Building on these findings, our study aimed to apply the principles of cocoa paste alkalinization, combined with the use of ultrasound, to valorize the residual biomass from the three most cultivated *Theobroma* species in the Amazon region. In this work, we hypothesized that variations in structure and composition among the *Theobroma* species may influence both the yield and nature of polysaccharide and non-polysaccharide components obtained through alkaline-assisted methods. Indeed, the pod husks of these *Theobroma* species differ markedly in the structure of the epicarp, mesocarp and endocarp. *T. cacao* features a thick, highly lignified epicarp that provides strong protection but limits extractability. In contrast, *T. grandiflorum* has a thinner, less lignified epicarp with a looser structure that enhances solvent penetration, while *T. bicolor* shows intermediate characteristics. The mesocarp of *T. cacao* is moderately dense and rich in pectic polysaccharides; *T. grandiflorum* presents a softer, more hydrated mesocarp with higher pectin solubility and *T. bicolor* exhibits a more fibrous yet less compact mesocarp, with a balanced polysaccharide composition. Lastly, the endocarp in *T. cacao* is thin and mucilaginous, contributing little to extractables, whereas *T. grandiflorum* has a more developed, pectin-rich endocarp and *T. bicolor* displays a less mucilaginous and more variable endocarp structure (Benlloch-Tinoco et al., 2024; Marasca et al., 2022; Oñate-Gutiérrez et al., 2023). Furthermore, regarding the biochemical composition, *T. cacao* husks are characterized by high levels of flavanols, particularly epicatechin and isoquercitrin, which contribute to their strong antioxidant potential. In contrast, *T. grandiflorum* husks exhibit a broader spectrum of flavonol compounds, including quercetin derivatives, reflecting a more diverse phenolic profile. Meanwhile, *T. bicolor* husks present a distinct composition marked by notable concentrations of myricetin and the presence of unique minor compounds such as scopoletin, highlighting species-specific differences in secondary metabolite profiles (Tauchen et al., 2016).

Additionally, we aimed to assess whether KOH could serve as an effective alternative to NaOH for alkaline extraction, potentially offering distinct advantages in terms of biopolymer composition and functionality. The two alkalis may interact differently with plant material, possibly due to the differing properties of their associated cations (K^+ vs Na^+), which may affect the solubility and swelling behavior of the plant matrix, as well as interact ionically in distinct ways with the polysaccharides embedded within the matrix (Gai et al., 2022; Safirzadeh et al., 2017). Notably, KOH has also been reported to offer economic benefits; according to Zhang et al. (Zhang et al., 2018), it generates <10 % of the wastewater produced by NaOH, significantly reducing treatment costs in plant processing operations.

In this work, we proposed US-assisted extraction to intensify the process, based on our previous study (Girón-Hernández et al., 2023a) which showed that US reduced the extraction temperature for pectic polysaccharides from apple pomace, achieving high yields while preserving bioactivity. Literature also highlights several benefits of US including: (1) improved mixing, (2) faster energy and mass transfer, (3) lower thermal and concentration gradients, and (4) increased yield and throughput (Hu et al., 2022; Liu et al., 2024).

2. Materials and methods

2.1.1. Materials

Dichloromethane (≥99.9 %), hydrochloric acid (ACS reagent, 37 %), 96 % ethanol, methanol (HPLC grade, ≥99.8 %), 3,5-dinitrosalicylic acid (DNS) reagent, Folin-Ciocalteu reagent, Biuret reagent (protein detection level 150–1000 μg/mL), potassium hydroxide (ACS reagent, ≥85 %), sodium carbonate (ACS reagent, 99.5 %), gallic acid, Trolox, quercetin (HPLC reagent ≥95 %), sugar standards (≥97 %), including galacturonic acid (GalA), glucuronic acid (GlcA), galactose (Gal), glucose (Glc), mannose (Man), xylose (Xyl), rhamnose (Rha) and arabinose (Ara), along with other chemicals such as acetonitrile, ammonium bicarbonate, ammonium hydroxide, formic acid and 3-(trimethylsilyl)-2,2,3,3-tetradeuteropropionic acid (TMSP-d4) were purchased from Merck, UK. Sodium hydroxide, deuterium oxide, 99.8 % (D_2O) and trifluoroacetic acid (TFA) were purchased from Fisher Scientific, UK. 1-Phenyl-3-methyl-5-pyrazolone (PMP) was supplied by Apollo Scientific, UK. Distilled water (dH_2O) water and MS-grade water were obtained from a Milli-Q® system (IQ 7005, Merck, UK).

2.1.2. Sample preparation

Fruits from three species were collected at the physiological ripeness stage (indicating full maturity through natural development on the plant, ~5–6 months) from the University of Amazonia's farm in Colombia. They were washed, dried and opened to separate seeds, funicle and pods. Pods were chopped, sun-dried to constant weight or oven-dried (40 °C, UF30, Memmert, Germany). The dried material was ground to ~200 μm using a MultiDrive Basic (IKA, Germany) and, then, stored in a desiccator.

2.1.3. Setup of the Design of Experiments (DoE) and extraction of biopolymers from pod husk powder

The optimization of the biopolymers extraction was conducted using Response Surface Methodology (RSM) with a Box-Behnken design. The factors studied were extraction time (Et, min), temperature (T, °C) and powder-to-solvent ratio (P, g/mL), systematically varied across 15 runs (Table S1), where factor levels ranged from 11.11 to 22.22 mg/mL for the powder-to-solvent ratio, 30–80 °C for temperature and 20–60 min for time. This design enabled the evaluation of linear and quadratic effects, as well as factor interactions. Replicates at the central condition (Et: 40 min, T: 55 °C, P: 0.016665 g/mL) to assess model reproducibility. For the extraction, the process followed the methodology reported by Gentile's group (Girón-Hernández, Rodríguez, et al., 2024), based on the combinations of the studied factors (Et, T, P). Pod husk powder was dissolved in a Duran glass flask with 45 mL of 0.05 M alkaline solution (NaOH or KOH) and heated to the target temperature in an ultrasonic bath (VWR, UK) at 45 kHz for the specified time. Phase separation of the coarse and diluted polymeric material was achieved by centrifugation at 3900 rpm for 30 min using a Sorvall ST1 Plus centrifuge (Thermo Fisher, UK). The supernatant was mixed with 96 % ethanol (1:1 vol/vol) and stored at 4 °C for 24 h to precipitate the polymers. After refrigeration, the mixture was centrifuged at 2000 rpm for 30 min to recover the polymer as a pellet. The polymer was then dialyzed in dH_2O using cellulose membrane tubing (molecular weight cut-off 12–14 kDa Merck, UK) for 48 h, with the water changed three times daily. Finally, it was dried on non-stick baking paper in a MIR-154 incubator (Panasonic, Japan) at 37 °C until constant weight and stored.

2.2. Analysis of the moisture and ash content

2.2.1. Moisture content

Moisture content was determined by drying the sample at 105 ± 2 °C to a constant weight and expressed as g/100 g, calculated as the ratio of water weight (wet weight minus dry weight) to wet weight.

2.2.2. Ash content

Ash content was measured by ashing samples in a muffle furnace ELF (Carbolite Gero Ltd., UK) at 550 ± 10 °C for 2 h and expressed as g/100 g, calculated as the ratio of ash weight to sample weight.

2.3. Color measurement

Color measurements were taken at five random points on both the lightest and darkest areas of the extracted materials using a DigiEye system (DigiPix, VeriVide, UK). A white standard plate was used for calibration and background. Results were expressed in CIE Lab color space (10° observer, D65 illuminant), with L* (lightness), a* (green-red), b* (blue-yellow) and automatically calculated chroma intensity (C*) and hue angle (h*).

2.4. Bioactive profile and antioxidant capacity

2.4.1. Total phenolics (TP) determination

TP was assessed using a modified Folin-Ciocalteu method (Macías-Garbett et al., 2022). A 50 µL sample (1 mg/mL) was mixed with 430 µL dH_2O and 20 µL Folin-Ciocalteu reagent. After adding 50 µL Na_2CO_3 (20 g/100 mL) and incubating in darkness for 10 min, the mixture was diluted with 450 µL dH_2O. A 200 µL aliquot was transferred to a 96-well plate and absorbance was measured at 680 nm (FLUOstar UV–Vis, BMG Labtech, Germany). A gallic acid equivalents (GAEq) calibration curve (0.05–1 mg/mL, $R^2 = 0.997$) was used, expressing results as mg GAE/g sample.

2.4.2. Total flavonoids (TF) determination

TF was quantified using the A319717-Plant Flavonoids Assay (Antibodies, UK). Samples (1 mg/mL) in 60 % ethanol were mixed with 15 µL nitrite solution (5 min), then 15 µL chromogen (5 min), followed by 120 µL NaOH and 90 µL 60 % ethanol (15 min). Absorbance at 502 nm was measured in a 96-well plate. A quercetin equivalents (QEq) calibration curve (0.0156–1 mg/mL, $R^2 = 0.999$) was used, with results as mg QEq/g sample.

2.4.3. Total oligomeric proanthocyanidins (TPA) determination

TPA was assessed using the A319718-Plant Oligomeric Proanthocyanidins Assay Kit (Antibodies, UK). Samples (1 mg/mL) in extraction buffer were mixed (40 µL sample + 160 µL reagent) in a 96-well plate and incubated at 30 °C for 30 min. Absorbance at 500 nm was measured. A catechin equivalents (CEq) standard curve (0.039–5 mg/mL, $R^2 = 0.996$) was used, with results as mg CEq/g sample.

2.4.4. Oxygen radical absorbance capacity (ORAC) determination

ORAC was measured using the ab233473-ORAC Assay Kit (Abcam, USA). Samples (0.02 mg/mL) in 1× assay diluent were mixed with 150 µL Fluorescein solution, incubated at 37 °C for 30 min and fluorescence (Ex/Em = 480/520 nm) recorded. After adding 25 µL Free Radical Initiator (80 mg/mL), fluorescence was recorded every min for 1 h. A Trolox equivalents (TEq) standard curve (0–50 µM, $R^2 = 0.991$) was used, with results in M TEq/g sample.

2.4.5. Ferric reducing antioxidant power (FRAP)

FRAP was assessed using the Ferric Antioxidant Status Detection Kit (Thermo Fisher Scientific, UK). Samples (1 mg/mL, 1:10 dilution) were mixed with 75 µL FRAP reagent in a 96-well plate and incubated for 30 min. Absorbance at 560 nm was measured. An ascorbic acid standard curve (0.05–1000 µM, $R^2 = 0.999$) was used, with results in mmol Fe^{2+}/g sample.

All measurements were performed in triplicate, at a minimum, following the manufacturer's specifications.

2.5. Analysis of metabolites by mass spectrometry (MS)

Pod powders (10 mg) were extracted in 1 mL analytical methanol, sonicated (15 min, ice-water bath) and centrifuged (15000 rpm, 15 min, 4 °C). Supernatants were vacuum-dried (45 °C, 2 h), resuspended in 100 µL 95/5 LC/MS-grade water/acetonitrile, sonicated and filtered (0.22 µm Costar Spin X, 10,000 rpm, 5 min). Filtrates were transferred to autosampler vials with 200 µL micro-inserts. Extraction blanks and pooled QCs were included for MS/MS exclusion/inclusion lists and stability assessment.

Chromatographic separation used a Waters HSS T3 column (2.1 mm × 150 mm, 1.7 µm, 35 °C, 250 µL min^{-1}). A binary buffer system (0.1 % ammonium hydroxide) followed a gradient of Buffer A (95/5 LC/MS-grade water/acetonitrile) and Buffer B (5/95): T0–1.5 min, 95 % A; T1.5–11.5 min, 5 % A; T15–20 min, 95 % A. Injection-to-injection time: 21.5 min. Data acquisition followed a data-dependent (Thermo AcquireX) approach. MS1: 30,000 resolution (100–1000 *m/z*, Quad RF 30, AGC 95 %, max injection 50 ms). MS2: stepped HCD (10, 35, 60), 1.0 m/z isolation. Metrics: vaporizer temp 275 °C, ion transfer tube 300 °C, gas flow (sheath: 35, aux: 7, sweep: 0). Data were converted to .abf files and aligned using Riken MSDial 4.9. MS2 matches (≥70 % similarity, 10-ppm tolerance) were verified with an authentic library. QC metrics (RSD ≤1.3 %, threshold ≤15 % in both modes) ensured stable MS/MS signals (RSD ≤25 %) with metadata: formula, S/N ratio, retention time, m/z, adduct, MS/MS match score and InChIKey.

2.6. Structural sugars determination

Structural sugar determination involved hydrolysis, derivatization and quantification, based on adaptations of existing methods (Slimestad et al., 2019). One milligram of extracted material was placed in a glass vial with 1000 µL dH_2O and 500 µL TFA (4 M). The sealed vial was heated at 120 °C with stirring for 90 min and then cooled. To remove

residual TFA, 200 μL of methanol was added and the mixture was evaporated at 80 °C. The resulting residue was re-dissolved in 1 mL dH_2O. For monosaccharide derivatization, 200 μL hydrolyzed solution was mixed with 80 μL 0.3 M NaOH and 80 μL PMP in methanol, The mixture was incubated at 80 °C for 60 min, cooled, neutralized with 80 μL 0.3 M HCl and diluted to 1 mL. Excess PMP was removed by extraction with CH_2Cl_2 (3 × 1 mL), followed by vortexing at 30,000 rpm for 30 s. All samples and sugar standards were derivatized, filtered (0.45 μm) and transferred to chromatographic vials. Sugar quantification was performed using UV detection (250 nm) on an ACQUITY Premier UHPLC with a single quadrupole MS. Separation was achieved on a C18 column (50 × 2.1 mm, 1.7 μm) at 25 °C, using ammonium bicarbonate/ammonium hydroxide (pH 9.2) and acetonitrile. Mass spectrometry was used to confirm the identity of peaks (ESI-MS, positive mode, 400–1000 *m/z*, 200 ms scan). Characteristic pseudomolecular ions included: 481 m/z (pentoses), 495 m/z (deoxy-hexoses), 511 m/z (hexoses) and 525 m/z (uronic acids). Data were processed using MassLynx software (v4.2). The rhamnogalacturonan-I (RG-I) domain content was estimated using the formula RG-I (%) ≈ 2Rha (mol%) + Ara (mol%) + Gal (mol%), while the homogalacturonan (HG) as GalA(mol%) − Rha (mol%) (Wu et al., 2023a).

2.7. Molecular weight determination

Molecular weight was determined by size-exclusion chromatography (Agilent, UK) using a Jasco PU-4180 pump, Kontron 480 column oven and Shodex RI-101 detector. The system included a 1× PL Aquagel-OH MIXED-H (8 μm, 50 × 7.5 mm) guard column and 2× PL Aquagel-OH MIXED-H (8 μm, 300 × 7.5 mm) columns. Samples (10 g/L) were dissolved in 0.2 M $NaNO_3$+ 0.01 M NaH_2PO_4 (pH 7), filtered (0.45 μm) and manually injected (20 μL, full-loop mode). The oven was set to 50 °C, pump pressure at 1.7 MPa. Molecular weights were calculated using Clarity GPC extension Software (v2.3) against a 10-point Agilent Pullulan calibration (Mw 340–700 kDa).

2.8. FTIR-ATR characterization and esterification degree determination

FTIR spectra and esterification degree (DE) were analyzed using FTIR-ATR (Frontier PerkinElmer Inc., UK). Samples were placed on the ATR accessory, recording signals (4000–550 cm^{-1}, 32 scans, 2 cm^{-1} resolution). For DE, 10 mg of dry material was re-suspended in 5 mL dH_2O (pH ~5.5), dried and analyzed. DE was calculated via Spectrum IR software (v10) following a published protocol (Dranca et al., 2020) using peak areas at 1780–1720 cm^{-1} (COOH) and 1640–1600 cm^{-1} (COO^-) as:

$$DE\ (\%) = \frac{Area\ of\ COOH}{Area\ of\ COOH + Area\ of\ COO^-} \times 100 \quad (1)$$

2.9. ^1H NMR measurement

The extracted material was analyzed using NMR spectroscopy. Saturated samples were prepared in 0.7 mL of D_2O, with TMSP-d4 added at 0.0 ppm as an internal reference. The ^1H NMR spectra were acquired at 80 °C using an Advance III HD 700 MHz spectrometer equipped with a Prodigy TCI probe (Bruker, UK). Each spectrum consisted of 128 scans and 32 K data points (transformed to 128 K). Baseline corrections were applied prior to integration. Data were processed by applying baseline corrections prior to integration, through Mnova software (v15.1). The degree of esterification has been calculated following the protocol reported by Grasdalen et al. (Grasdalen et al., 1988a) that is related to the intensities (I) of the line patterns A and B by the formula:

$$DE\ (\%) = \frac{I_A - I_B}{I_A + I_B} \times 100 \quad (2)$$

where B refers to the signals from H-5 of charged units and A corresponds to the signals from H-1 and H-5 of esterified units.

2.10. Thermal analysis

The thermal performance of the extracted materials was analyzed using a Thermogravimetric Analyzer (TGA 1 STARe System, Mettler-Toledo, Switzerland). Each test sample (~6 mg) was heated at a rate of 10 °C/min from room temperature (25 °C) to 800 °C in a nitrogen gas environment with a flow rate of 10 mL/min. Furthermore, the thermal properties were evaluated by Differential Scanning Calorimetry (DSC) using the DSC 1 STARe System analyzer (Mettler-Toledo, Switzerland). Approximately 5 mg samples of each extracted materials were sealed in aluminum pans. The samples were heated from 30 °C to 450 °C at a rate of 10 °C/min. All tests were conducted under a nitrogen atmosphere with a flow rate of 10 mL/min. Results were normalized to the sample weight to allow for comparative analysis using the STARe Software (v18.0).

2.11. Rheology test

Sample solutions (2 % *w*/w) were solubilized in dH_2O under stirring (25 °C, 16 h) and rested overnight at 4 °C before rheological tests. Measurements were conducted using an MCR302 stress-controlled rheometer (AntonPaar GmbH, Austria) with 25 mm parallel plates. A water trap prevented dehydration and temperature was controlled via a Peltier system. Viscosity was measured at shear rates from 0.1 to 100 1/s (1 % strain), while frequency sweep tests used angular frequencies (100–0.1 rad/s, 1 % strain). Tests were performed in triplicate (Girón-Hernández et al., 2023b) and analyzed using the manufacturer's RheoCompass software (v1.3).

2.12. Multivariant analysis

In the statistical processing, dimensionality reduction was performed and a multivariate Principal Component Analysis (PCA) was applied to the evaluated variables: molecular weight, thermal properties at different temperatures (DSCT1, DSCT2), phenolics, flavonoids, proanthocyanidins, FRAP, ORAC, galacturonic acid content (GalA) and degree of esterification (DE). The analyzed samples included CC-NaOH and CC-KOH (derived from *T. cacao*), GF-NaOH and GF-KOH (*T. grandiflorum*), BC-NaOH and BC-KOH (*T. bicolor*), and COM-P (commercial pectin used as control). A 10-variable × 7-sample data matrix was created for this purpose. The analysis was conducted using R software (v4.5.1).

3. Results and discussion

3.1. Analysis of Theobroma species pod husk

The harvested fruits of the three *Theobroma* species had fresh weights of ~1 kg or more (up to ~1.5 kg), with *T. bicolor* being the heaviest, followed by *T. grandiflorum* and *T. cacao*. Upon separating the fruit components, *T. cacao* showed a residual husk mass ratio 1.5 folder more than both *T. bicolor* and *T. grandiflorum*. Table 1 shows the average fresh

Table 1
Fresh weight distribution of fruit components of *T. cacao* (CC), *T. grandiflorum* (GF) and *T. bicolor* (BC).

Species	Fresh fruit (g)	Seeds (g)	Funiculus (g)	Pod husk (g)	Total fruit (g)	Pod/Fruit ratio
CC	103.3 ± 12.6	151.7 ± 7.6	30.0 ± 5.0	661.7 ± 22.5	946.7 ± 22.5	0.70 ± 0.01
GF	385.0 ± 55.0	236.7 ± 34.0	98.3 ± 15.3	653.3 ± 119.3	1373.3 ± 200.4	0.47 ± 0.04
BC	396.7 ± 107.5	290.0 ± 105.0	56.67 ± 2.9	740.0 ± 160.0	1483.3 ± 370.0	0.50 ± 0.02

weights of each fruit and its component after seed removal. The husks of *T. bicolor* were the hardest, while both *T. grandiflorum* and *T. cacao* had softer husks.

Moisture and ash content analyses of fresh and dry pods revealed significant variations among the species, with implications for industrial processing (Table S2). The high moisture content observed in fresh *T. cacao* pods (84.61 ± 0.86 %) suggests a greater capacity for water retention, consistent with prior studies of its its hydration potential (Djali et al., 2021; Dos Anjos Lopes et al., 2023). While this trait may help maintain freshness, it also increases drying time and energy consumption, posing challenges for industrial scalability. In contrast, the lower moisture contents of *T. grandiflorum* and *T. bicolor* (72.13 ± 1.14 % and 75.12 ± 2.47 %, respectively), are aligned with literature highlighting their lower water retention, making them more cost-efficient for drying processes (Benlloch-Tinoco et al., 2024). Regarding ash content, fresh *T. cacao* pods had the highest mineral concentration (4.36 ± 0.12 %), making them promising for biofertilizer production, as reported in studies emphasizing the value of mineral-rich byproducts in soil amendment (van Vliet & Giller, 2017). Conversely, the low ash content in fresh *T. grandiflorum* pods (0.66 ± 0.09 %) makes them better suited for pectin extraction, where minimal mineral interference is desired. This observation is supported by existing research (Kazemi et al., 2021), which suggests that low ash content aids in producing high-purity pectin in accordance with FAO standards for food additive specifications (Joint FAO/WHO Expert Committee on Food Additives, 2006). Notably, this trend is reversed in dry pods, with *T. grandiflorum* exhibiting the highest ash content (9.43 ± 0.21 %).

Differences in fresh and dry weights, along with drying yields, underscore the variability in biomass utilization across species. *T. cacao* pods, with a fresh weight of 596.67 ± 116.23 g and a dry yield of 27.07 ± 1.44 %, reflect their high initial moisture and lower drying efficiency, in line with previous findings. In contrast, *T. grandiflorum* pods demonstrated greater efficiency with a similar fresh weight of 606.67 ± 85.05 g but a substantially higher dry yield (54.37 ± 3.97 %), highlighting their suitability for sustainable biomass processing. *T. bicolor* showed the highest fresh weight (765.33 ± 165.91 g) and an

A

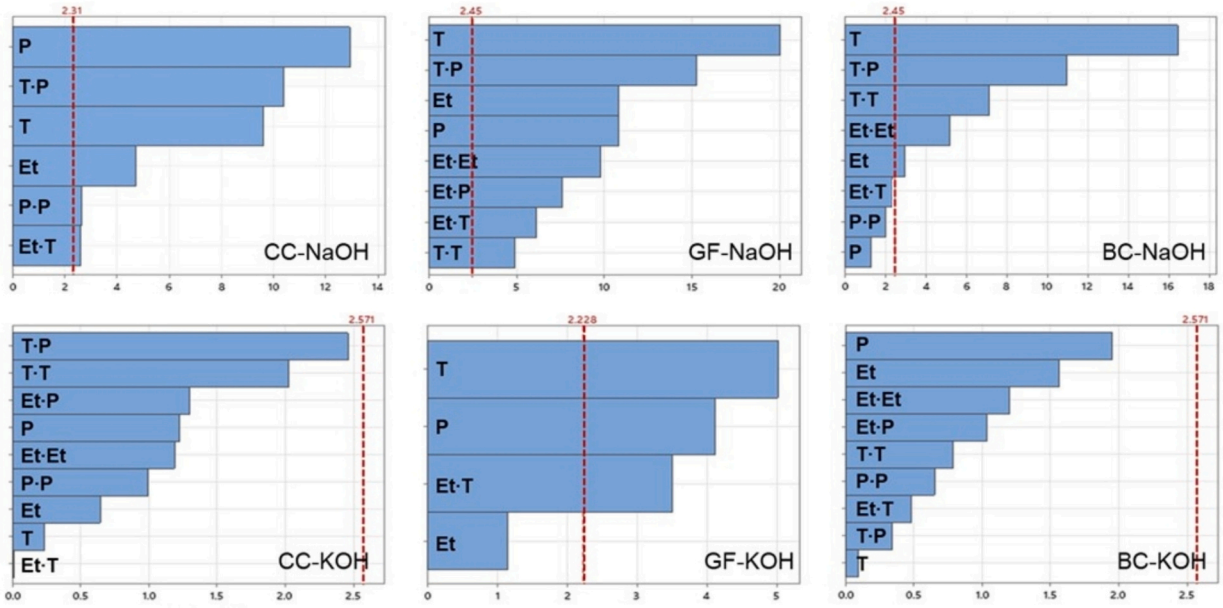

B

Sample	Regression equations for biopolymers yield extraction in uncoded units	R^2 (%)	R^2 Adj (%)	R^2 Pred (%)	Pred. Value (%)	Obs. Value (%)	Error (%)
CC-NaOH	= 63.7 + 0.3 Et - 0.8 T - 1668 P - 53934 P·P - 0.003 Et·T + 45 T·P	98.1	96.6	91.2	40.7	38.0	7.2
CC-KOH	= 53 + 0.13 Et + 0.5 T - 4694 P - 0.005 Et·Et - 0.006 T·T + 57927 P·P + 0.00005 Et·T + 20.3 Et·P + 30.6 T·P	76.7	34.6	0.0	23.7	23.0	3.0
GF-NaOH	= -5.2 + 0.2 Et + 0.1 T + 486 P - 0.002 Et·Et + 0.0005 T·T + 0.001 Et·T - 4.5 Et·P - 7.2 T·P	99.5	98.7	95.1	8.7	8.0	8.5
GF-KOH	= 8.8 - 0.1 Et - 0.04 T - 153.1 P + 0.002 Et·T	84.8	78.7	65.7	11.1	5.0	122
BC-NaOH	= 7.2 + 0.2 Et - 0.04 T + 261 P - 0.002 Et·Et + 0.002 T·T + 9317 P·P - 0.0006 Et·T - 10.8 T·P	98.8	97.2	91.1	14.9	14.7	1.5
BC-KOH	= 5.5 - 0.3 Et + 0.2 T + 540 P + 0.002 Et·Et - 0.001 T·T - 15933 P·P - 0.001 Et·T + 6.7 Et·P - 1.8 T·P	67.5	9.0	0.0	11.1	10.6	4.6

Fig. 1. Pareto charts of standardized effects (x-axis) of factors (y-axis)-temperature (T), extraction time (Et), pods powder/solvent ratio (P) and interactions- on the extraction yield (%). Bars crossing the red dashed line indicate significance (α = 0.05) (A). Fitted model equations and metrics: coefficient of determination (R^2), adjusted coefficient of determination (R^2 Adj.), predictive coefficient of determination (R^2 Pred.), the predicted extraction yield (Pred. Value), observed extraction yield (Obs. Value) and the experimental percentage error (Error), calculated as difference between the predicted and observed values, divided by the observed value (%) (B).

intermediate dry yield (48.69 ± 2.08 %) (Table S3), representing a balance profile between water content and biomass retention, making it versatile for diverse applications.

3.2. Biopolymer extraction from Theobroma species using NaOH and KOH

After characterizing the different waste biomass (exocarp) from the *Theobroma* genus, biopolymer extraction was performed using NaOH and KOH as solvents, with temperature (T), extraction time (Et) and pods powder/solvent ratio (P) as factors. Results revealed marked differences in extraction performance between NaOH and KOH, likely due to variations in the solubility of pectic-related compounds, material composition, or distinct chemical interactions with the alkaline solutions. Significant factors or their interactions (crossing the red dashed line) were identified using a Pareto chart (Fig. 1A), with non-influencing factors retained only if they interacted with key factors. This underscores the complex dependency on factor interactions for the extraction. Response surface methodology provided insights into process efficacy, model reliability and predictive performance (Fig. 1B). Overall, among the factors considered in the DoE for NaOH extractions across all species, temperature consistently emerged as a key variable, highlighting its role in the biopolymers solubilization. The pods powder/solvent ratio also ranked highly, particularly in *T. cacao* and *T. grandiflorum*, highlighting its importance in optimizing yield. Conversely, KOH exhibited poor performance, with no factors identified as significant in several cases, indicating weaker chemical interactions and limited extraction efficiency. For *T. cacao* with NaOH, powder/solvent ratio significantly influenced yield, both as an independent factor (P, P·P) and through its interaction with temperature (T·P). The model showed excellent reliability with all metrics >90 % and the predicted yield (40.7 %) closely aligned with the observed yield (38.0 %), with an extraction error of 7.2 %. KOH extraction, however, revealed no significant factors, with limited model reliability, though predicted and observed yields were similar (23.7 % vs. 23.0 %). *T. grandiflorum* produced the lowest yields for both treatments. With NaOH, temperature was the dominant factor, followed by its interaction with the pods powder/solvent ratio (T•P), extraction time (Et) and the ratio itself (P). The model achieved high accuracy, all metrics >95 %, with predicted (8.7 %) and observed yields (8.0 %) showing an 8.5 % error. KOH extractions had a simplified model, with T remaining dominant, followed by P and Et•T. While moderate reliability, presenting metrics in the range of (65 % to 85 %), a 122 % extraction error indicated a large discrepancy between predicted (11.1 %) and observed yields (5 %). For *T. bicolor* with NaOH, T was the most influential factor, alongside interactions (T•P, T•T). The model showed high accuracy with all coefficients >91 %, with predicted (14.9 %) and observed yields (14.7 %) closely matching and a minimal error (1.5 %). With KOH, results mirrored those of *T. cacao*, although the factors were not significant, they were retained to ensure statistical completeness.

The findings confirm that temperature significantly influences pectin solubilization in *Theobroma* species, aligning with literature emphasizing its role in enhancing reaction kinetics and breaking down protopectin complexes. Elevated temperatures hydrolyze mainly ether and ester bonds, releasing soluble pectic polysaccharides (Qian et al., 2021). Optimal extraction temperatures (70–90 °C) balance yield with functional property preservation, such as methoxylation and esterification (Girón-Hernández et al., 2023b). However, regardless of the solvent applied during extraction, excessive heat may affect the functional properties of extracting biopolymers, lowering molecular weight and gel-forming ability, as reported in the literature for pectic polysaccharides, which become less suitable for applications requiring specific viscoelastic properties (Said et al., 2023). In NaOH extractions, temperature enhances solvent penetration, disrupting cell matrices and releasing bound pectin (Sandarani, 2017). Studies on sunflower heads and sugar beet pulp confirm temperature accelerates pectin solubilization while maintaining high yields and purity (Muñoz-Almagro et al., 2023; Peighambardoust et al., 2021).

Higher extraction yields with NaOH stem from its strong base strength, effectively breaking down plant cell walls and solubilizing protopectin (Abang Zaidel et al., 2017). KOH, though milder, preserves functional properties, producing cleaner extracts but with slightly lower yields (Iglesias & Lozano, 2004). NaOH's aggressive action also extracts impurities, requiring further purification, whereas KOH retains more structural integrity, minimizing contamination (Iglesias & Lozano, 2004).

3.3. Moisture and ash content measurement

For the moisture content of the extracted materials (Table S4), *T. cacao* exhibited the lowest value in both treatments (NaOH: 4.17 ± 0.53 %, KOH: 3.03 ± 0.61 %), indicating lower water retention capacity compared to the other species. In contrast, *T. bicolor* showed the highest values (NaOH: 7.11 ± 1.14 %, KOH: 5.42 ± 0.66 %), suggesting higher water retention, which could influence extraction processes and final product properties. *T. grandiflorum* exhibited intermediate values (NaOH: 5.75 ± 1.45 %, KOH: 4.93 ± 1.35 %), indicating similar behavior to *T. bicolor*, even with lower water retention capacity.

Regarding ash results, *T. cacao* showed the highest ash content with KOH treatment (3.77 ± 0.60 %), indicating a higher mineral concentration. *T. grandiflorum* exhibited the lowest ash values across both treatments (NaOH: 3.01 ± 0.31 %, KOH: 2.58 ± 0.30 %), making it more suitable for applications requiring low mineral content, such as the food industry, where ash levels must be controlled. *T. bicolor* had intermediate ash values, higher than *T. grandiflorum* but lower than *T. cacao*, with 3.47 ± 0.16 % in NaOH and 3.07 ± 0.13 % in KOH, indicating a moderate mineral concentration.

3.4. Color measurement

NaOH extraction produces darker samples than KOH, with *T. cacao* and *T. bicolor* showing reddish hues and *T. grandiflorum* a yellowish hue. Fig. 2A illustrates the color variations of the extracted materials by source and method. Notably, cocoa husk extraction with NaOH shifts the hue angle from 333.89° (blue) to 38.40° (red-orange) (Fig. 2B), as consequence of the different content of phenolic compounds (par. 3.5).

3.5. Bioactive profile and antioxidant capacity

Fig. 3A summarizes assay results, while Fig. 3B compares normalized bioactive profiles and antioxidant capacity. NaOH extraction increased phenolics, flavonoids and proanthocyanidins in *T. cacao* and *T. bicolor* pod husks. *T. grandiflorum* showed stable bioactive content, though proanthocyanidins were higher with KOH (1580 ± 250 mg CEq/g). *T. bicolor* (NaOH) had the highest bioactive profile: 460 ± 9 mg GAEq/g phenolics, 328 ± 5 mg QEq/g flavonoids and 2090 ± 880 mg CEq/g proanthocyanidins.

These results contrast with prior findings on *T. bicolor* seed husks (Baldera Ocampo et al., 2021; Vázquez-Ovando et al., 2015), likely due to differences in sample treatment. Vázquez-Ovando et al. analyzed defatted pod husks, while Ocampo et al. used hot-water infusion extracts. Extracted material is notable, as its pulp has higher reported values. This may reflect the pod husk's structural role, which may not require high secondary metabolite content for fruit protection (Jean-Marie et al., 2022; Mar et al., 2024; Sanchez-Ballesta et al., 2022).

The *Theobroma* samples exhibited higher bioactive content than commercial citrus pectin (90 ± 6 mg GAEq/g phenolics, 37 ± 3 mg QEq/g flavonoids, 1040 ± 158 mg CEq/g proanthocyanidins). However, proanthocyanidins assays have limitations, as non-specific reactions with dihydrochalcones, anthocyanins, flavan-3-ols and ascorbic acid can lead to overestimation (Waterman & Mole, 1994). Factors such as solvent acidity, proanthocyanidins concentration and temperature

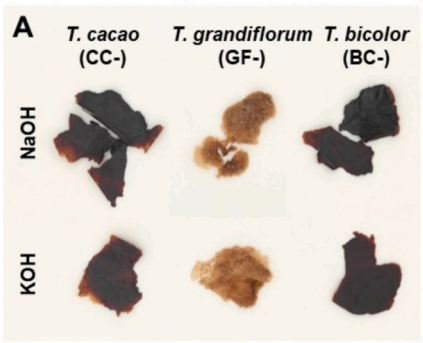

B

Sample	Area	L*	a*	b*	C*	h°
CC-NaOH	L	27.53±0.22	0.84±0.09	-0.41±0.15	0.95±0.09	333.89±8.99
	D	42.13±2.14	13.12±2.47	11.11±2.38	20.95±9.17	38.40±8.65
CC-KOH	L	29.12±0.92	7.06±2.91	0.08±0.60	7.10±2.96	350.99±8.95
	D	51.26±3.47	16.01±4.78	17.27±6.04	23.10±6.14	46.99±6.78
GF-NaOH	L	44.53±3.52	16.00±1.89	24.55±2.15	29.33±2.49	56.93±2.76
	D	63.29±6.04	15.13±4.10	33.89±5.07	37.19±5.95	66.12±4.11
GF-KOH	L	52.89±2.76	20.54±1.15	36.50±1.27	41.88±1.66	60.91±0.53
	D	78.30±1.68	7.81±0.80	29.40±0.89	30.42±1.05	75.15±1.05
BC-NaOH	L	22.25±3.11	1.13±0.30	-0.16±0.05	1.15±0.31	348.28±6.89
	D	38.93±3.06	15.84±3.44	8.91±4.18	21.05±6.18	38.34±2.49
BC-KOH	L	28.92±3.97	6.18±2.70	1.00±2.03	5.07±3.20	16.74±9.42
	D	61.36±5.53	12.45±3.11	7.41±1.91	17.20±8.48	61.68±6.55

Fig. 2. (A) Images of the materials extracted from *T. cacao*, *T. bicolor* and *T. grandiflorum* using NaOH and KOH. (B) Average values and standard deviations of color coordinates, chroma and hue measured on both the lightest and darkest areas of the extracted materials.

A

	Bioactive profile			Antioxidant capacity	
Sample	Phenolics[1]	Flavonoids[2]	Proathocyanidins[3]	FRAP[4]	ORAC[5]
CC-NaOH	360±7	195±53	2450±406	127.82±6.44	3.26±0.1
CC-KOH	172±19	156±11	1630±365	56.28±4.65	3.03±0.1
GF-NaOH	170±18	57±6	1160±128	32.56±3.78	2.59±0.1
GF-KOH	152±4	65±12	1580±250	31.92±0.77	2.52±0.1
BC-NaOH	460±9	328±5	2090±880	232.69±1.09	2.18±0.1
BC-KOH	320±20	270±20	1570±117	157.31±4.90	1.75±0.1
COM-P	90±6	37±3	1040±158	27.44±0.89	2.93±0.0

Values are expressed as equivalents (Eq) on a dry basis: [1]mg GAEq/g, [2]mg QEq/g, [3]mg CEq/g, [4]mmol Fe^{2+}/g, [5]M Trolox Eq/g

B

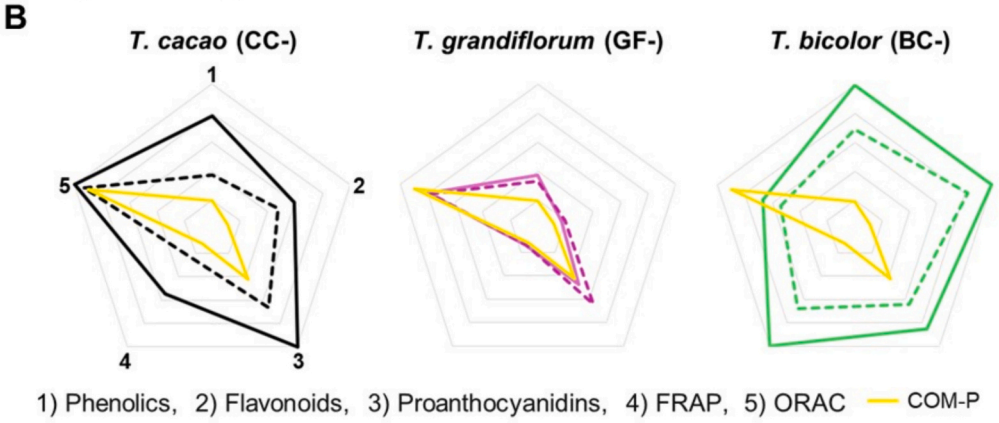

Fig. 3. Bioactive profile and antioxidant capacity of the extracted polysaccharides (A). Comparative representation of normalized data, illustrating differences between sample sources and extraction methods with NaOH in solid line and KOH in dashed line (B). Commercial citrus pectin (COM-P) is included as a reference.

fluctuations further impact accuracy (Sun et al., 1998; Waterman & Mole, 1994). Regarding the antioxidant activity, NaOH extractions yielded higher FRAP values than KOH, particularly in cocoa (127.8 ± 6.4 vs. 56.3 ± 4.7 mmol Fe^{2+}/g) and *T. bicolor* (232.7 ± 1.1 vs. 157.3 ± 4.9 mmol Fe^{2+}/g). Commercial pectin (27.4 ± 0.9 mmol Fe^{2+}/g) exhibited lower reducing power than most extracts, except for *T. grandiflorum*, highlighting NaOH's superior extraction efficacy. ORAC values showed smaller differences, with NaOH slightly outperforming KOH in cocoa (3.3 ± 0.1 vs. 3.0 ± 0.1 M Trolox/g) and *T. bicolor* (2.2 ± 0.1 vs. 1.8 ± 0.1 M Trolox/g). For *T. grandiflorum*, differences were negligible. Commercial pectin (2.9 ± 0.01 M Trolox/g) exhibited comparable or higher ORAC values, suggesting its antioxidant profile favors radical scavenging over reducing power.

Comparisons of these values should consider limited literature on *Theobroma* pectic materials and variations in extraction analysis methods (Benlloch-Tinoco et al., 2024). Also, proanthocyanidin content may be influenced by sample color (Mannino et al., 2021), while the Folin-Ciocalteu assay may overestimate phenolics due to contributions from non-phenolic reducing agents (Munteanu & Apetrei, 2021).

These findings indicate that alkaline extraction (0.05 M), particularly NaOH, is advantageous for preserving phenolics better than acidic or microwave-assisted methods (Mellinas et al., 2020), likely due to reduced heat-related degradation (~70 °C vs. ~100 °C in microwave extractions).

3.6. Metabolomic profiling of extracted material

The analysis revealed that both solvents enabled the extraction of comparable metabolite pools. However, all extractions performed using NaOH resulted in the detection of >200 metabolites, whereas in KOH-

based extractions, this threshold was surpassed only in the case of *T. grandiflorum* (Table S5). Metabolites were classified into ten main functional groups, along with an additional "others" category (Fig. 4). Fatty acids emerged as the dominant class, ranging from 48 % in CC-KOH up to 81 % in GF-NaOH extracted materials, in agreement with their key role as major constituents of plant cell membranes (Reszczyńska & Hanaka, 2020). Carboxylic acids represented the second most abundant group (up to 19.4 % in the CC-KOH extract). Indeed, intermediate compounds such as citric, succinic and maleic acids were detected. These compounds likely reflect residual metabolic activity or degradation products (Supplementary material-Metabolite list). Interestingly, amino acids were also prominently identified, with KOH extractions favoring a higher recovery of this group (17.5 % for CC-KOH). Notably, tyrosine, tryptophan and phenylalanine were recovered in significant quantities (Table S5), consistent with their well-established role as precursors in polyphenol biosynthesis. Tyrosine serves as a central precursor in antioxidant biosynthesis pathways (Marchiosi et al., 2020).

Furthermore, direct detection of phenolic compounds in the extracted materials was noteworthy (relative abundance from 2.7 to 6.2 %), considering their bioactive potential and their reported contribution to cytocompatibility in our previous studies (Girón-Hernández, Tombe, et al., 2024). These phenolic constituents may also enhance the cross-linking efficiency of polysaccharide-based formulations (Pan et al., 2024). Among them, p-coumaric acid was prominently detected, aligning with its role in the phenylpropanoid biosynthetic pathway responsible for polyphenol production. Alkaloids were also identified (from 0.12 to 0.99 %), as expected for the studied genus, with trigonelline, theobromine and caffeine being the most representative. These compounds are well known for their stimulant properties, particularly in *Theobroma* species (Jazayeri et al., 2021). Finally, a similar relative abundance (up to ~0.5 %) of vitamins, nucleic acids and hormones was detected because of the transformation processes induced by the extraction treatment. Notably, within the other compounds category, traces of serotonin were observed, potentially originating from the metabolic transformation of tryptophan present in the extracted material (Walther et al., 2003).

3.7. Structural sugars, monosaccharides composition

The sugar composition of pectic materials from *Theobroma* species varied based on extraction method (NaOH vs. KOH) (Fig. 5A). KOH extraction preserved more rhamnose, a key component of rhamnogalacturonan-I (Davis et al., 1990). In *T. cacao*, rhamnose

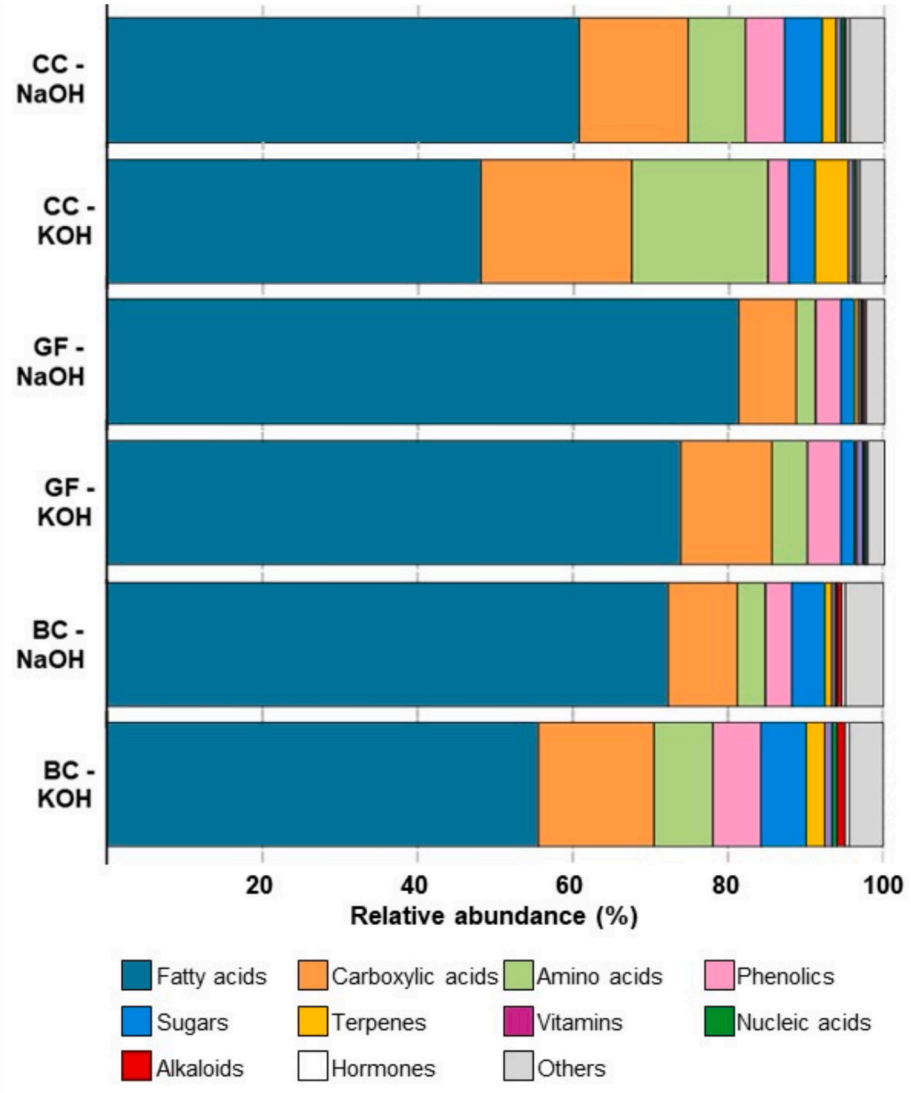

Fig. 4. Relative abundance (%) of metabolite classes identified in samples treated with NaOH and KOH from three different *Theobroma* matrices based on metabolomic analysis.

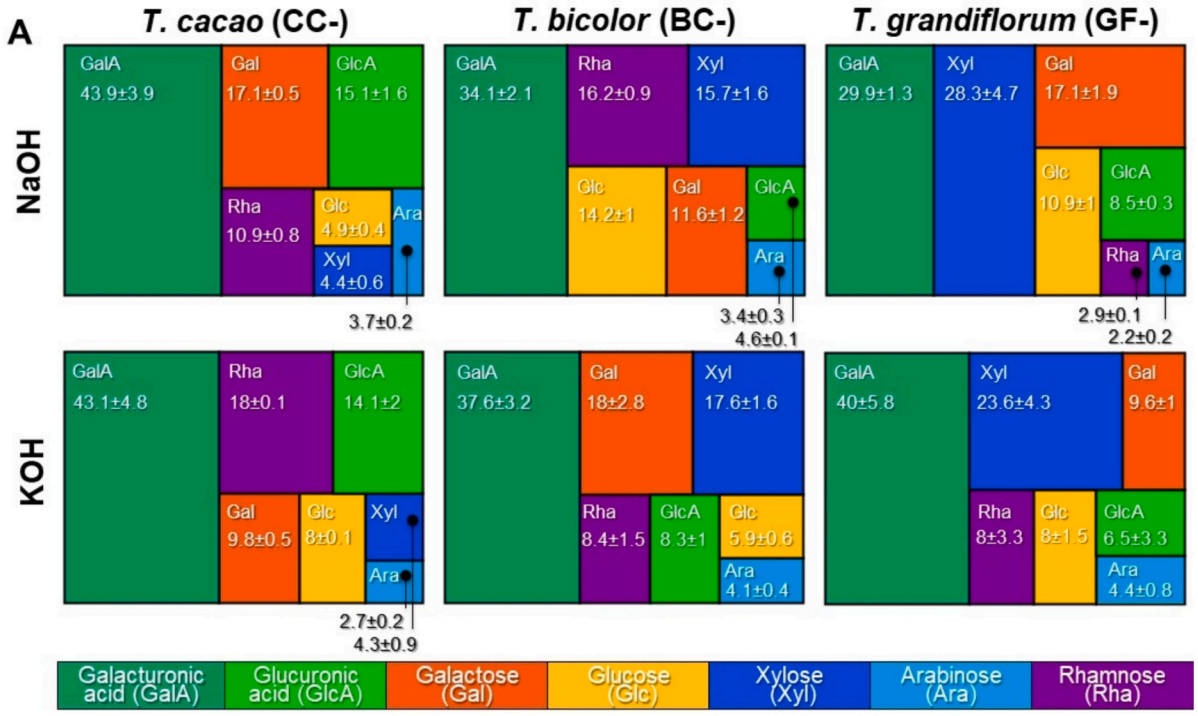

B

	CC-NaOH	CC-KOH	BC-NaOH	BC-KOH	GF-NaOH	GF-KOH
HG (%)	33.0±4.0	25.1±4.8	17.9±2.3	29.2±3.5	27.0±1.3	32.0±6.7
RG-I (%)	42.6±1.3	48.5±0.7	47.4±2.2	39.0±3.5	25.1±1.9	30.0±4.7

Fig. 5. (A) Structural sugar composition (%) of the polysaccharides extracted from the different *Theobroma* genus biomasses using NaOH and KOH alkaline treatments, analyzed by UHPLC. (B) Table reporting the corresponding calculated values (%) for the homogalacturonan (HG) and rhamnogalacturonan I (RG-I) domains. The homogalacturonan (HG) domain content was estimated as GalA(mol%) − Rha (mol%) while the rhamnogalacturonan-I (RG-I) using the formula RG-I (%) ≈ 2Rha (mol%) + Ara (mol%) + Gal (mol%).

increased from 10.9 % (NaOH) to 18 % (KOH), while galactose decreased from 17.1 % to 9.8 %, that may be related to the presence of different pools of extracted polysaccharides. In *T. grandiflorum*, KOH yielded higher galacturonic acid (40 % vs. 29.9 % with NaOH) and lower galactose (9.6 % vs. 17.1 %), while *T. bicolor* showed a similar trend, with higher galacturonic acid (37.6 % vs. 34.1 %) but lower glucose and rhamnose.

The calculated proportions of the RG-I and HG domains are reported in Fig. 5B. As reported in the literature, Rha content plays a key role in defining the primary structure of pectic polysaccharides. The RG-I domain backbone is composed of repeating GalA and Rha units; therefore, a higher Rha content reflects a longer RG-I chain. The side chains, primarily consisting of neutral sugars such as Gal and Ara, are interwoven and attached to the backbone, forming the RG-I domain (Vincken et al., 2003). Notably, the materials BC-NaOH and CC- both NaOH and KOH treatment had significantly higher Rha content, corresponding to the highest RG-I domain proportions, compared with materials extracted from *T. grandiflorum*. This structural feature can be associated with an increased presence of bioactive compounds, such as flavonoids (Fig. 3A).

Furthermore, HG is a linear polymer made up of α-1,4-linked D-galacturonic acid units, which can carry varying degrees of methoxycarbonyl substitutions. In our work, CC-NaOH showed the highest proportions of the HG domain (~33 %) similar to results reported by Wu et al. (Wu et al., 2023b) that have extracted pectic polysaccharides from citrus segment membranes.

Species-specific differences in sugar composition were notable. *T. grandiflorum* exhibited particularly high xylose content (28.3 % with NaOH and 23.6 % with KOH), indicating a greater presence of xylan, xyloglucan or xylogalacturonan structures compared to *T. cacao* and *T. bicolor*. These polysaccharides, along with cellulose and lignin, contribute to the strength and resilience of fruit pods, providing mechanical protection and aiding the plant's defense against herbivores, damage and pathogens (Munzert & Engelsdorf, 2024). These structural features are crucial for seeds or pods that must withstand harsh environmental conditions before germination.

3.8. Molecular weight measurement

Fig. 6A illustrates the molecular weight (Mw) profiles of the different fragments of the samples extracted from the *Theobroma* species pod husks. Regardless of the fruit type and both alkaline conditions, all extracted pectic polysaccharides exhibited a bimodal Mw distribution. Notably, in all the samples, the first fragment to appear in the SEC elution profile (Peak 1) exhibited the highest Mw, where the highest Mw (783 kDa) was observed in the material extracted from *T. cacoa* after using NaOH as extraction solvent, while the lowest Mw (92.5 kDa) was found in the *T. grandiflorum* extract obtained with KOH. Regarding the remaining fragments (Peak 2 and Peak 3), the estimated Mw ranged between ~9 and ~37 kDa.

Furthermore, the molecular weight distribution of the extracted pectic polysaccharides is presented in Fig. 6B, highlighting distinct

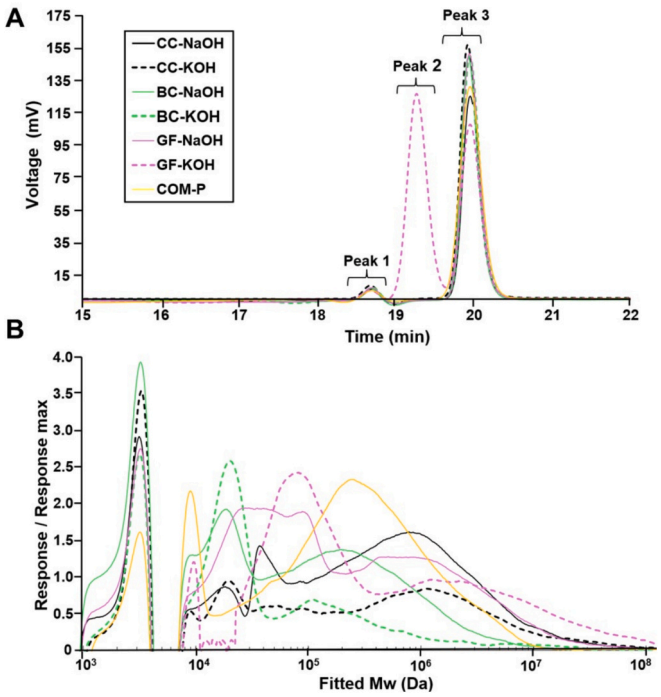

Fig. 6. Chromatographic SEC profiles of extracted pectic polysaccharides and COM-P (A) and the associated Mw distribution (B).

differences in their Mw profiles. The calculated values are available in the supplementary material (Table S6). As control, the commercial citrus pectin exhibited a predominantly high-Mw population (513 kDa), accounting for ~91.5 % of the total signal.

In contrast, the biopolymers extracted from *Theobroma* species demonstrated more complex Mw distribution, with up to 3 distinct populations. Such multimodal patterns have been consistently reported in the literature across various plant sources (Benito-Román et al., 2024; Li et al., 2019). Among the three species, *T. bicolor* yielded the lowest Mw values, followed by *T. grandiflorum* and *T. cacao*. Notably, KOH extraction resulted in a higher proportion of low-MW fractions in *T. bicolor* (20.5 kDa, ~78.8 % relative area) and *T. grandiflorum* (92.5 kDa, ~61.6 % relative area). Conversely, *T. cacao* showed a predominance of high-Mw materials under both extraction methods: 1069.5 kDa (~85.9 % area) and 1567.1 kDa (~76.8 % area) for KOH-extracted samples. However, the high polydispersity index (PDI > 1.7) in these samples suggests a broad distribution of molecular sizes. The commercial citrus pectin, despite having a single dominant peak, showed an even higher PDI (>2.2), indicating an even more heterogeneous mixture of molecular weights.

3.9. ^{1}H NMR measurement

To elucidate the structural features of the materials extracted from *Theobroma* species, ^{1}H NMR spectroscopic analysis was performed at 80 °C. This temperature was selected to reduce sample viscosity and improve resolution, thereby enabling more accurate chemical shift assignment, particularly for anomeric proton environments. The

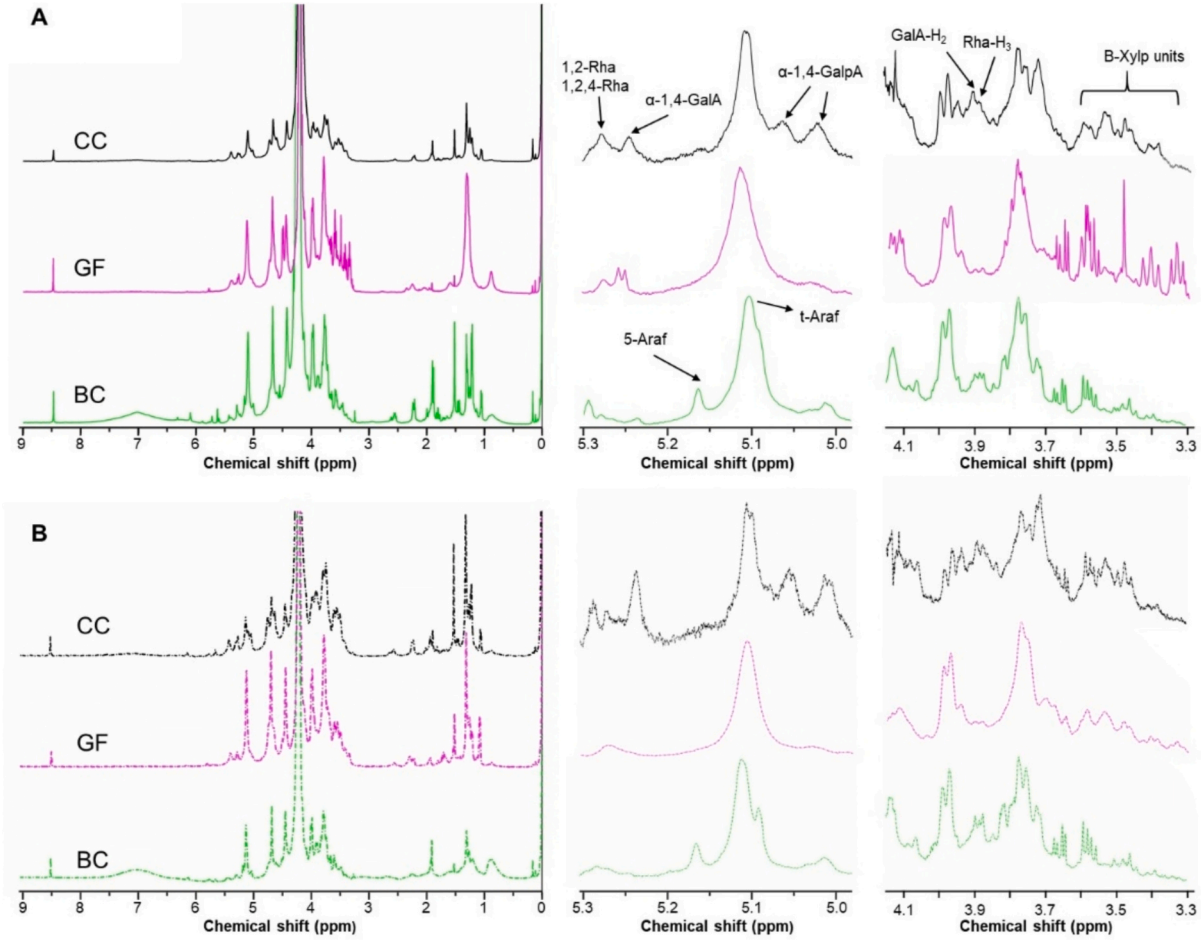

Fig. 7. ^{1}H NMR spectra (700 MHz) of the extracted materials, showing the full spectra (left of each panel) and expanded regions corresponding to the chemical shifts δ 5.3–5.0 ppm (middle) and δ 4.1–3.3 ppm (right). Panel (A) shows the NaOH-extracted materials, while panel (B) corresponds to the KOH-extracted materials.

anomeric region (5.5–4.3 ppm) of the spectra exhibited well-defined resonances that are characteristic of typical glycosidic linkages present in pectic and hemicellulosic polysaccharides. Notably, the signal at 5.28 ppm, corresponding to the α-(1 → 4)-linked oligomers of galacturonic acid (Hachem et al., 2016) was clearly identified in all extracted samples (Fig. 7). In contrast, the resonance at 4.55 ppm, attributed to β-(1 → 4)-linked oligomers of galacturonic acid, was detected only in the BC-NaOH sample.

The signal at 5.27 ppm, attributed to the anomeric proton of rhamnose residues involved in both 1,2- and 1,2,4-linkages (indicative of branched rhamnogalacturonan regions), was most prominent in the GF-NaOH, CC-KOH and BC-KOH extracts. A closely related signal at 5.25 ppm was observed in the CC-NaOH and BC-NaOH samples, likely representing the same structural motif. The slight shift in chemical shift may reflect differences in the local conformational environment of the rhamnose residues, such as variations in hydrogen bonding, ionic interactions or chain flexibility and hydration (Shi et al., 2017). The signal at 5.17 ppm, characteristic of internal α-(1 → 5)-linked arabinofuranosyl (Araf) residues in a linear arabinan or branched α-Araf substituted at O-3 or O-2, was exclusively observed in the BC-NaOH and BC-KOH spectra, indicating a unique structural feature in the polysaccharides extracted from *T. bicolor*; while an intense peak in the range of 5.10–5.12 ppm was detected across all extracts and was assigned to terminal α-(1 → 5) arabinofuranosyl residues (non-reducing end α-L-arabinofuranosyl) (Konishi et al., 2006). Furthermore, in CC-NaOH and CC-KOH samples, a distinct signal at 5.06 ppm was assigned to α-(1 → 4)-linked galactopyranosyl (GalpA) uronic acid. This was accompanied by minor resonances at 5.04 and 5.01 ppm, which were less apparent in the other samples and may reflect local variation in glycosidic environments or branching patterns (Colquhoun et al., 1990).

Additional signals corresponding to ring protons of α-galacturonic acid residues were consistently observed across all extracts. The H-5 resonance appeared at 4.67 ppm, H-4 at 4.43 ppm and H-2 at ~3.90 ppm (Hotchkiss et al., 2023). The H-3 signal was found near 4.11 ppm but partially overlapped with the residual D_2O peak and adjacent resonances from rhamnose units. The H-3 proton of α-rhamnose was assigned to a signal at 3.87 ppm. The H-6 methyl protons of rhamnose appeared as doublets centered at 1.23 and 1.30 ppm in all samples, except for GF-NaOH, where a single peak was observed at ~1.30 ppm. Interestingly, the ratio of substituted (1,2,4-Rha) to unsubstituted (1,2-Rha) rhamnose ranged from 5.5:1 for CC-NaOH to 1.1:1 for BC-NaOH, based on the integration of the H6,6′ signals at 1.22 and 1.29 ppm, respectively.

These resonances are attributed to rhamnose residues linked via (1 → 2) glycosidic bonds to galacturonic acid, as well as (2 → 1)-linked rhamnose units bearing O-4-substituted galacturonic acid branches, structural features consistent with rhamnogalacturonan-I (RG-I) domains (Huamani-Palomino et al., 2023). Additionally, two distinct signals between 2.0 and 2.2 ppm were assigned to acetyl groups attached at the 2-O and 3-O positions of GalA residues (Bédouet et al., 2003). Peaks in the 3.3–3.6 ppm range were attributed to the H-2, H-3, H-4 and H-5 protons of β-xylopyranose (β-Xylp) units, with higher intensities observed in the materials extracted from *T. grandiflorum* and *T. bicolor* (Patova et al., 2021). The H-1 of β-1.4-xylopyranosyl units typically appears between 4.4 and 4.5 ppm; however, its proximity to the H-4 signal of galacturonic acid may result in spectral overlap. Finally, a resonance at 8.5 ppm was detected in all the extracts. This signal is indicative of aromatic protons from phenolic compounds (Kontogianni et al., 2013). The presence of this signal suggests the co-extraction or retention of aromatic phenolics, potentially from cell wall-bound polyphenols, during the alkaline extraction process.

The degree of esterification (DE) of the extracted materials was determined via ^{1}H NMR using the method developed by H. Grasdalen et al. (Grasdalen et al., 1988b), resulting in a DE ranging from of 38.09 % calculated for CC-NaOH to 22.65 % for GF-KOH (Table S7) where the extractions in NaOH revealed higher DE.

3.10. FTIR-ATR characterization and esterification degree determination

Fig. 8 the FTIR-ATR spectra of extracted materials and commercial pectin, revealing similar peaks across all samples. A broad band at 3313 cm^{-1} corresponds to hydroxyl group stretching, while the 2925 cm^{-1} band, prominent in commercial pectin, represents C—H bending vibrations (CH, CH_2, CH_3). Other signals in this range result from O—H stretching due to hydrogen bonding in carboxyl groups (Ghoshal & Negi, 2020). The broad O—H absorption highlights intermolecular hydrogen bonds, affecting galacturonic acid's hydroxyl groups (Gnanasambandam & Proctor, 2000). As a result, O—CH_3 activity is masked by hydroxyl groups, making it unreliable as an indicator of methoxylation (Ghoshal & Negi, 2020), masking O—CH_3 activity as a methoxylation indicator.

The esterified carboxyl group (COOR) appears at 1725 cm^{-1}, supporting the presence of pectic polysaccharides in the extracted materials. The 1800–1500 cm^{-1} spectral region was crucial for determining DE via FTIR, with 1725 cm^{-1} (C═O stretching) and 1610 cm^{-1} (COO— asymmetrical stretching) indicating carboxylic ester and acid groups (Manrique & Lajolo, 2002). Using Chatjigakis' method (Chatjigakis et al., 1998), DE ranged from 25.6 % (GF-KOH) to 38.8 % (CC-NaOH), aligning with ^{1}H NMR results (Table S7).

Below 1430 cm^{-1}, characteristic pectin bands at 1313, 1230 and 1145 cm^{-1} correspond to methyl groups, C—H bending and C—O—C stretching in the pyranose ring that is part of the structure of the sugars that make up pectin (Pereira et al., 2016) and hemicellulose polysaccharides (Peng & Wu, 2010).

Furthermore, FTIR-ATR analysis revealed that each extracted material exhibits a distinct absorption maximum within the 1200–900 cm^{-1} range (Fig. 8B). This spectral region is primarily influenced by ring vibrations, along with contributions from C—OH stretching and C—O—C glycosidic bond vibrations. Notably, bands at ~1070 and ~ 1043 cm^{-1} can be attributed to rhamnogalacturonan, consistent with previous reports (Kacuráková et al., 2000). However, a band at 1072 cm^{-1} was also characteristic of β-galactan, that is associated to pectic polysaccharide. Also, a slight peak observed at 1066–1064 cm^{-1} can be assigned to the β-(1 → 4)-mannan, a typical component of hemicellulosic polysaccharides (Kacuráková et al., 2000). Commercial pectin differs in band shape due to industrial extraction and raw material variation, as pectin's structural properties depend on feedstock and isolation methods (Chan & Choo, 2013).

3.11. Differential scanning calorimetry (DSC) and thermo-gravimetric analysis (TGA)

DSC measurements were conducted for each extracted sample and compared with the analysis of a commercial pectin (Fig. 9A). The thermograms of all samples revealed similar behavior, highlighting the presence of exothermic and endothermic peaks (Table S8). The broad endothermic peaks, observed in the range from 146.2 °C for GF-KOH to 169.6 °C for BC-NaOH, indicated weight loss due to the vaporization of water. Similarly, Siqueira et al. (Siqueira et al., 2022) identified an endothermic peak at 132 °C in films produced of pectin extracted from *C. brasiliense* mesocarp. Interestingly, the materials extracted using NaOH presented higher endothermic peaks, resulting more comparable to the commercial counterpart. Exothermic peaks were observed in the range from 237.1 °C for CC-KOH to 267.0 °C for BC-NaOH, reflecting decomposition caused by pectic polysaccharides chain degradation. Nisar et al. reported exothermic decomposition temperatures ranging from 231.53 °C to 234.88 °C for citrus pectin films containing clove essential oil (Nisar et al., 2018). Similarly, Cervera et al. (Cervera et al., 2004) and Chaudhari and Singhal (Chaudhari & Singhal, 2015) observed peaks between 200 °C and 300 °C, associating them with characteristic polymeric decomposition.

Fig. 9B presents on the top the TGA thermographs, illustrating the weight loss trend as a function of temperature, while on the bottom it displays the DTG thermographs, highlighting the maximum thermal

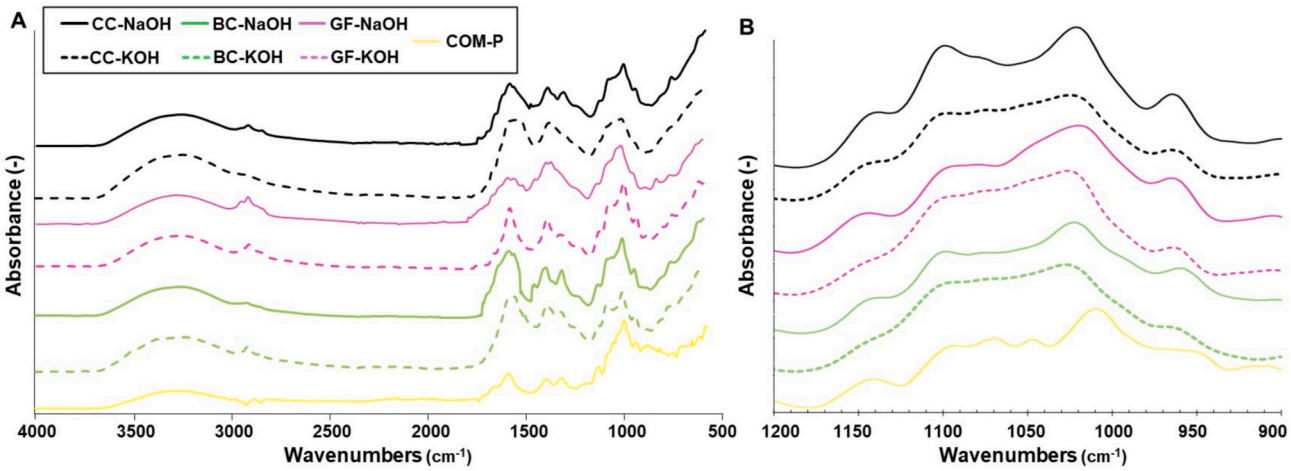

Fig. 8. FTIR-ATR spectra of the biopolymers extracted from the *Theobroma* genus recorded in the mid-infrared range (4000–550 cm^{-1}) (A) and in the 1200–800 cm^{-1} region for the identification of monosaccharides with different structures and compositions (B). COM-P refers to the commercial pectin.

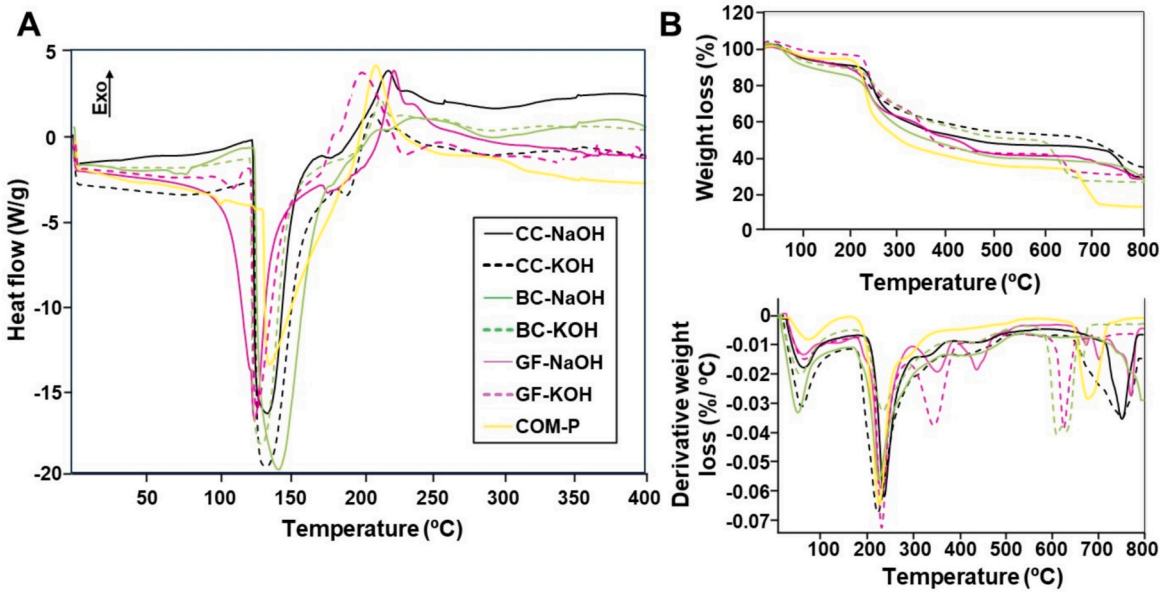

Fig. 9. Thermal characterization of the extracted materials and the commercial pectin: (A) DSC thermograms and (B) TGA (top) and DTG curves (bottom).

degradation temperature (T_{max}) for the extracted polysaccharides and commercial pectin. The TGA traces display similar mass loss patterns demonstrating comparable resistance to thermal degradation that occurred in four distinct stages. The first stage took place from room temperature up to 115 °C, with a T_{max} ranging from 70 °C for GF-KOH and to 74.2 °C for CC-NaOH (Table S9) and ~6 % weight loss.

The first stage corresponds to the loss of free water weakly bound to the polymer, facilitated by pectin's hydrophilic nature, aligning with Nešić et al. (Nešić et al., 2017). The second stage (185–260 °C), visible in all the extracted materials, showed a T_{max} from 235.0 °C (CC-KOH) to 243.4 °C (CC-NaOH) with a 30 % weight loss, that can be attributed to the decomposition of pectic polysaccharides (Wang et al., 2016). Additionally, a third stage (285–400 °C), more pronounced in the materials extracted from *T. grandiflorum* (both extraction methods) and *T. cacao* (using NaOH), exhibited degradation peaks around 350 °C and 420 °C, with weight loss ranging from 40 % (*T. cacao*) to 58 % (*T. grandiflorum*). These peaks can be attributed to the decomposition of the hemicellulosic polysaccharides (Werner et al., 2014).

Beyond 500 °C, mass loss slowed as remaining char degraded, confirmed by exothermic heat flow traces. Notably, *T. grandiflorum* materials degraded at lower temperatures (640–675 °C) than *T. cacao* (750–755 °C). All extracted materials exhibited thermal behavior like commercial pectin but with higher residual char at 800 °C (~40 % vs. ~18 %), likely due to residual hemicelluloses and celluloses.

3.12. Rheological analysis

Rheological analysis showed distinct behaviors between *Theobroma*-derived materials and commercial pectin (COM-P, Merck). Fig. 10A illustrates viscosity as a function of shear rate, where all solutions exhibited shear-thinning behavior, typical of pectin solutions due to polymer chain alignment under shear stress (Chan et al., 2017).

CC-NaOH and CC-KOH displayed the highest viscosity, suggesting *T. cacao* materials form a highly structured, viscous network, likely due to high molecular weight and strong intermolecular interactions. COM-P had the lowest viscosity, highlighting the superior rheological performance of NaOH-extracted samples.

Frequency sweep tests at 25 °C showed GEL behavior ($G' > G''$) for all solutions, including COM-P (Fig. 10B). At higher frequencies (>50 rad/s), BC-KOH exhibited SOL behavior ($G' < G''$), indicating a transition in

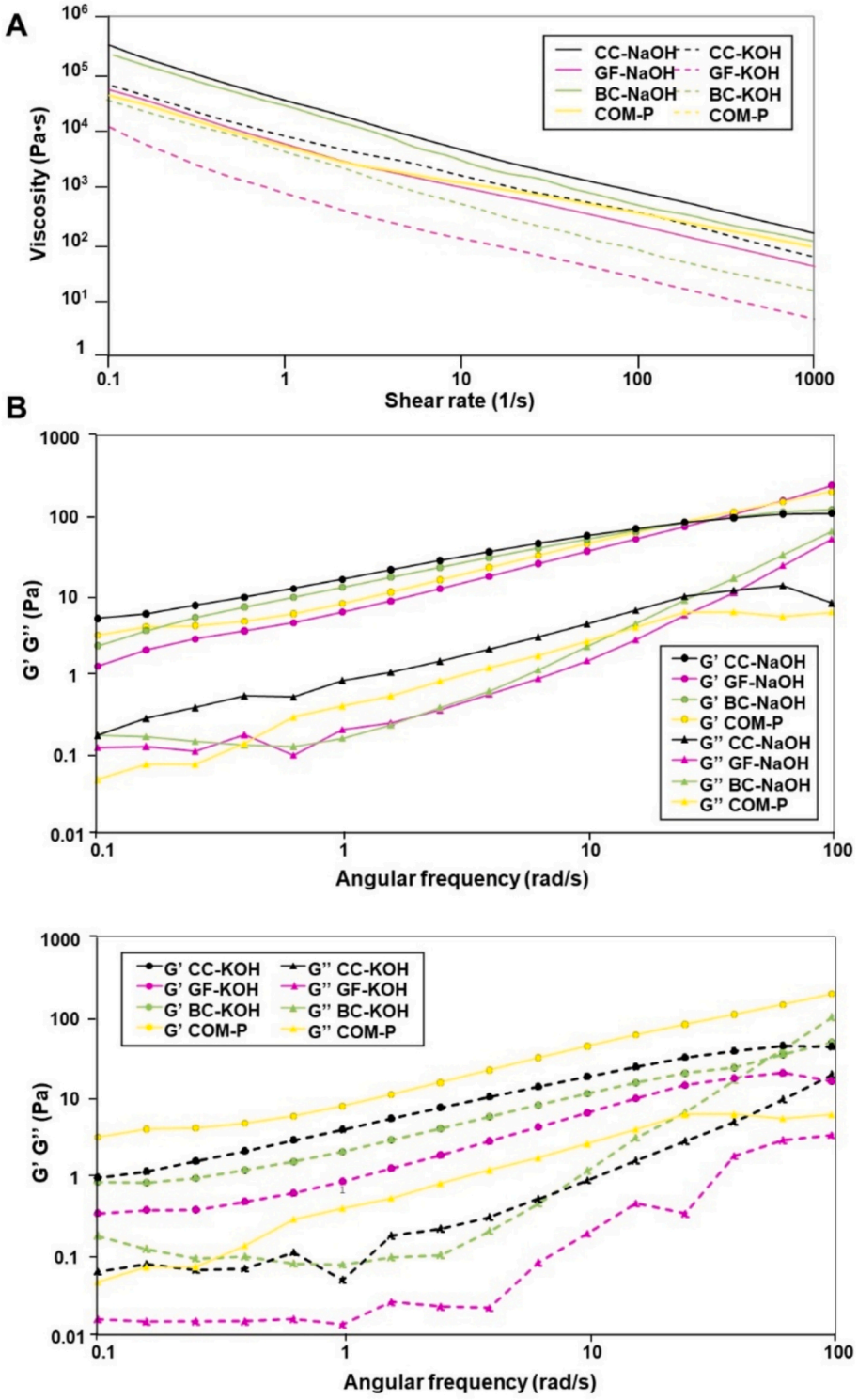

Fig. 10. (A) Flow-curves and (B) rheological properties obtained from frequency sweep tests of the solutions prepared from the extracted materials. Citrus pectin from Merck (COM-P) has been used as control.

mechanical properties. The extraction process significantly influenced solution behavior, possibly because of the higher content of bioactive compounds, with NaOH-extracted *T. cacao* and *T. bicolor* materials achieving higher viscosity. These findings suggest that *T. cacao*-derived materials are most suitable for applications requiring high viscosity and strong gel structures, *T. bicolor* materials are ideal for moderate viscosity needs and *T. grandiflorum* materials are better suited for applications requiring more fluid-like properties. The choice of biomass and extraction method can be tailored to optimize materials functionality for specific industrial uses.

3.13. Multivariant analysis

Principal Component Analysis (PCA) of samples showed that PC1 and PC2 accounted for 76.4 % of the variance (Fig. 11). PC1 was driven by GalA content, molecular weight (Mw) and degree of esterification

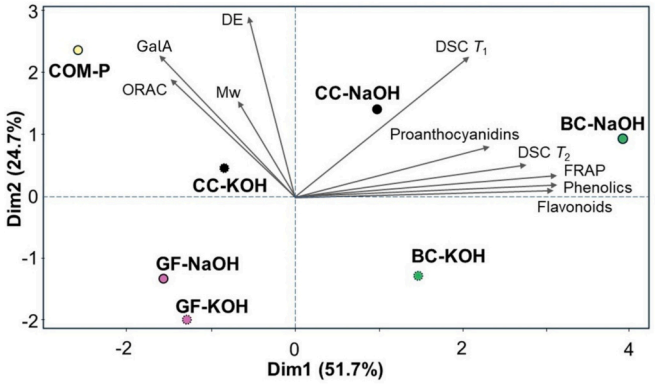

Fig. 11. Principal Component Analysis (PCA) biplot illustrating the distribution of pectin samples and the contribution of the evaluated variables.

(DE), while PC2 reflected antioxidant activities (ORAC, FRAP) and thermal properties (DSC). The scores plot revealed distinct clustering, with higher DE and Mw samples separating from lower values, emphasizing their impact on samples behavior. The loadings analysis confirmed GalA, Mw and DE strongly correlated with PC1, defining structural properties, while PC2 was linked to antioxidant activity and thermal stability, suggesting extraction influences these attributes. Mw and DE showed a positive correlation, while variations in ORAC and FRAP indicated structural modifications affecting radical scavenging properties.

Higher DSC values corresponded to altered thermal stability due to molecular interactions from chemical modifications. The correlation between Mw, DE and GalA supports their role in solubility and gelation, consistent with studies emphasizing esterification and molecular weight in the extracted materials functionality.

4. Conclusion

This study examined polysaccharides extraction from *T. cacao* (CC), *T. grandiflorum* (GF) and *T. bicolor* (BC) using NaOH and KOH, revealing significant differences in yield, bioactivity and functionality. *T. bicolor* (NaOH) exhibited the highest bioactive content, antioxidant activity and diverse metabolomic profile, including amino acids, phenolics and alkaloids, enhancing its therapeutic potential. *T. cacao* (NaOH) had the highest molecular weight (~783 kDa) and viscosity, ideal for gel-forming applications requiring structural stability and *T. cacao* (KOH) had the highest galacturonic acid content (43 %). NaOH extraction generally yielded higher bioactive compounds (e.g. phenolics) content and structural integrity, while KOH preserved homogalacturonan integrity, offering distinct functional advantages. The extraction yields varied by species and solvent, with *T. cacao* (NaOH) showing the highest recovery, whereas *T. grandiflorum* had the lowest. Compared to commercial citrus pectin, *T. bicolor* and *T. cacao* materials exhibited superior bioactive profiles, molecular weights and gel-forming properties. Their antioxidant properties exceeded commercial pectin, making them suitable for nutraceutical and pharmaceutical applications. Enhanced viscosity, gel strength and superior thermal stability in *T. cacao* and *T. bicolor* suggest their feasibility in industrial applications requiring heat resistance. These findings highlight *Theobroma* polysaccharides as functional material, offering tailored physicochemical and bioactive properties for specific applications. However, this study has some limitations, including the lower extraction efficiency observed with KOH and the high variability in biomass composition among *Theobroma* species, which may affect process reproducibility. Moreover, the need for further purification and standardization constrains immediate scalability. Future research should focus on optimizing downstream processing to improve purity and evaluating bioactivity in application-specific models. In particular, the antioxidant, prebiotic and anti-inflammatory properties of the extracts warrant investigation for their potential use in functional foods and tissue engineering applications.

Supplementary data to this article can be found online at https://doi.org/10.1016/j.carbpol.2025.124070.

CRediT authorship contribution statement

Jose Manuel Núñez-Ramírez: Writing – original draft, Methodology, Investigation, Formal analysis. **Andrea Martelli:** Writing – original draft, Methodology, Investigation, Formal analysis. **Tabitha Halliday:** Writing – original draft, Methodology, Investigation, Formal analysis. **Bradley Thomas:** Methodology, Investigation, Formal analysis. **Corinne Wills:** Methodology, Investigation, Formal analysis. **Valeria Cannillo:** Writing – review & editing, Supervision. **Devis Bellucci:** Writing – review & editing, Supervision. **Carlos Carranza:** Resources, Investigation, Funding acquisition, Formal analysis. **Paola A. García-Rincón:** Supervision, Project administration. **Piergiorgio Gentile:** Writing – review & editing, Supervision, Resources, Methodology, Investigation, Funding acquisition, Formal analysis, Conceptualization. **Joel Girón-Hernández:** Writing – review & editing, Writing – original draft, Supervision, Resources, Project administration, Methodology, Investigation, Funding acquisition, Formal analysis, Conceptualization.

Declaration of Generative AI and AI-assisted technologies in the writing process

In the preparation of this work, the author(s) used ChatGPT 4 for assistance with proof-editing. After utilizing this tool/service, the author (s) carefully reviewed and revised the content as needed, assuming full responsibility for the final publication.

Declaration of competing interest

The authors declare that they have no known competing financial interests or personal relationships that could have appeared to influence the work reported in this paper.

Acknowledgements

This work was supported by the NERC Cross-disciplinary Research for Discovery Sciences (NE/X018229/1) and the Ministerio de Ciencia, Tecnología e Innovación, Colombia (project BPIN 2021000100065). The authors particularly acknowledge the funding provided by Colombia, which sponsored the research secondments of J. Núñez, C. Carranza and P.A. García-Rincón at Northumbria University and Newcastle University in the UK.

Data availability

Data will be made available on request.

References

Abang Zaidel, D. N., Hamidon, N. H., & Mat Zahir, N. (2017). Extraction and characterization of pectin from sweet potato (*Ipomoea batatas*) peels using alkaline extraction method. *Acta Horticulturae, 1152*. https://doi.org/10.17660/ActaHortic.2017.1152.29

Baldera Ocampo, J. F., Granda Santos, M. S., & Chavez Quintana, S. G. (2021). Capacidad antioxidante y polifenoles totales de infusión de cascarilla de cacao (Theobroma cacao) y macambo (Theobroma bicolor). *Revista de Investigación de Agroproducción Sustentable, 5*(3). https://doi.org/10.25127/aps.20213.814

Barrios-Rodríguez, Y. F., Salas-Calderón, K. T., Orozco-Blanco, D. A., Gentile, P., & Girón-Hernández, J. (2022). Cocoa pod husk: A high-pectin source with applications in the food and biomedical fields. *ChemBioEng reviews, 9*(5). https://doi.org/10.1002/cben.202100061

Bédouet, L., Courtois, B., & Courtois, J. (2003). Rapid quantification of O-acetyl and O-methyl residues in pectin extracts. *Carbohydrate Research, 338*(4). https://doi.org/10.1016/S0008-6215(02)00500-1

Benito-Román, Melgosa, R., Illera, A. E., Sanz, M. T., & Beltrán, S. (2024). Kinetics of extraction and degradation of pectin derived compounds from onion skin wastes in

subcritical water. *Food Hydrocolloids, 153*, Article 109957. https://doi.org/10.1016/J.FOODHYD.2024.109957
Benlloch-Tinoco, M., Nuñez Ramírez, J. M., García, P., Gentile, P., & Girón-Hernández, J. (2024). *Theobroma* genus: Exploring the therapeutic potential of *T. grandiflorum* and *T. bicolor* in biomedicine. *Food Bioscience, 61*, Article 104755. https://doi.org/10.1016/J.FBIO.2024.104755
Cervera, M. F., Heinämäki, J., Krogars, K., Jörgensen, A. C., Karjalainen, M., Colarte, A. I., & Yliruusi, J. (2004). Solid-state and mechanical properties of aqueous chitosan-amylose starch films plasticized with polyols. *AAPS PharmSciTech, 5*(1). https://doi.org/10.1007/bf02830583
Chan, S. Y., & Choo, W. S. (2013). Effect of extraction conditions on the yield and chemical properties of pectin from cocoa husks. *Food Chemistry, 141*(4). https://doi.org/10.1016/j.foodchem.2013.06.097
Chan, S. Y., Choo, W. S., Young, D. J., & Loh, X. J. (2017). Pectin as a rheology modifier: Origin, structure, commercial production and rheology. *Carbohydrate Polymers, 161*. https://doi.org/10.1016/j.carbpol.2016.12.033
Chatjigakis, A. K., Pappas, C., Proxenia, N., Kalantzi, O., Rodis, P., & Polissiou, M. (1998). FT-IR spectroscopic determination of the degree of esterification of cell wall pectins from stored peaches and correlation to textural changes. *Carbohydrate Polymers, 37*(4). https://doi.org/10.1016/S0144-8617(98)00057-5
Chaudhari, S. A., & Singhal, R. S. (2015). Cutin from watermelon peels: A novel inducer for cutinase production and its physicochemical characterization. *International Journal of Biological Macromolecules, 79*. https://doi.org/10.1016/j.ijbiomac.2015.05.006
Colquhoun, I. J., de Ruiter, G. A., Schols, H. A., & Voragen, A. G. J. (1990). Identification by n.m.r. spectroscopy of oligosaccharides obtained by treatment of the hairy regions of apple pectin with rhamnogalacturonase. *Carbohydrate Research, 206*(1), 131–144. https://doi.org/10.1016/0008-6215(90)84012-J
Davis, E. A., Derouet, C., Herve Du Penhoat, C., & Morvan, C. (1990). Isolation and an N. M.R. study of pectins from flax (linum usitatissimum L.). *Carbohydrate Research, 197* (C), 205–215. https://doi.org/10.1016/0008-6215(90)84143-I
Djali, M., Kayaputri, I. L., Kurniati, D., Sukarminah, E., Mudjenan, I. M. H., & Utama, G. L. (2021). Degradation of lignocelluloses cocoa shell (*Theobroma cacao* L.) by various types of mould treatments. *Journal of Food Quality, 2021*. https://doi.org/10.1155/2021/6127029
Dos Anjos Lopes, S. M., Martins, M. V., de Souza, V. B., & Tulini, F. L. (2023). Evaluation of the nutritional composition of cocoa bean shell waste (*Theobroma cacao*) and application in the production of a phenolic-rich iced tea. *Journal of Culinary Science and Technology, 21*(5). https://doi.org/10.1080/15428052.2021.2016531
Dranca, F., Vargas, M., & Oroian, M. (2020). Physicochemical properties of pectin from Malus domestica 'Fălticeni' apple pomace as affected by non-conventional extraction techniques. *Food Hydrocolloids, 100*, Article 105383. https://doi.org/10.1016/J.FOODHYD.2019.105383
Febrianto, N. A., & Zhu, F. (2022). Comparison of bioactive components and flavor volatiles of diverse cocoa genotypes of Theobroma grandiflorum, Theobroma bicolor, Theobroma subincanum and Theobroma cacao. *Food Research International, 161*. https://doi.org/10.1016/j.foodres.2022.111764
Gai, L., Ren, E. F., Tian, W., Niu, D., Sun, W., Hang, F., & Li, K. (2022). Ultrasonic-assisted dual-alkali pretreatment and enzymatic hydrolysis of sugarcane bagasse followed by Candida tropicalis fermentation to produce xylitol. *Frontiers in Nutrition, 9*, Article 913106. https://doi.org/10.3389/FNUT.2022.913106/BIBTEX
Ghoshal, G., & Negi, P. (2020). Isolation of pectin from kinnow peels and its characterization. *Food and Bioproducts Processing, 124*. https://doi.org/10.1016/j.fbp.2020.09.008
Girón-Hernández, J., Pazmino, M., Barrios-Rodríguez, Y. F., Turo, C. T., Wills, C., Cucinotta, F., … Gentile, P. (2023a). Exploring the effect of utilising organic acid solutions in ultrasound-assisted extraction of pectin from apple pomace, and its potential for biomedical purposes. *Heliyon, 9*(7), Article e17736. https://doi.org/10.1016/J.HELIYON.2023.E17736
Girón-Hernández, J., Pazmino, M., Barrios-Rodríguez, Y. F., Turo, C. T., Wills, C., Cucinotta, F., … Gentile, P. (2023b). Exploring the effect of utilising organic acid solutions in ultrasound-assisted extraction of pectin from apple pomace, and its potential for biomedical purposes. *Heliyon, 9*(7). https://doi.org/10.1016/j.heliyon.2023.e17736
Girón-Hernández, J., Rodríguez, Y. B., Corbezzolo, N., Blanco, D. O., Gutiérrez, C. C., Cheung, W., & Gentile, P. (2024). Exploiting residual cocoa biomass to extract advanced materials as building blocks for manufacturing nanoparticles aimed at alleviating formation-induced oxidative stress on human dermal fibroblasts. *Nanoscale Advances, 6*(15), 3809–3824. https://doi.org/10.1039/d4na00248b
Girón-Hernández, J., Tombe, A., Chemban Koyilot, M., Salas-Calderón, K. T., Charlton, A., Wills, C., & Gentile, P. (2024). From cocoa waste to sustainable bioink: Valorising pectin for circular economy-driven tissue engineering. *European Polymer Journal, 210*, Article 112967. https://doi.org/10.1016/J.EURPOLYMJ.2024.112967
Gnanasambandam, R., & Proctor, A. (2000). Determination of pectin degree of esterification by diffuse reflectance Fourier transform infrared spectroscopy. *Food Chemistry, 68*(3). https://doi.org/10.1016/S0308-8146(99)00191-0
Grasdalen, H., Einar Bakøy, O., & Larsen, B. (1988a). Determination of the degree of esterification and the distribution of methylated and free carboxyl groups in pectins by 1H-n.m.r. spectroscopy. *Carbohydrate Research, 184*(C), 183–191. https://doi.org/10.1016/0008-6215(88)80016-8
Grasdalen, H., Einar Bakøy, O., & Larsen, B. (1988b). Determination of the degree of esterification and the distribution of methylated and free carboxyl groups in pectins by 1H-n.m.r. spectroscopy. *Carbohydrate Research, 184*(C). https://doi.org/10.1016/0008-6215(88)80016-8
Hachem, K., Benabdesslem, Y., Ghomari, S., Hasnaoui, O., & Kaid-Harche, M. (2016). Partial structural characterization of pectin cell wall from Argania spinosa leaves. *Heliyon, 2*(2), Article e00076. https://doi.org/10.1016/J.HELIYON.2016.E00076
Hotchkiss, A. T., Chau, H. K., Strahan, G. D., Nuñez, A., Harron, A., Simon, S., … Yeom, H. W. (2023). Carrot rhamnogalacturonan i structure and composition changed during 2017 in California. *Food Hydrocolloids, 137*, Article 108411. https://doi.org/10.1016/J.FOODHYD.2022.108411
Hu, W., Cheng, H., Wu, D., Chen, J., Ye, X., & Chen, S. (2022). Enhanced extraction assisted by pressure and ultrasound for targeting RG-I enriched pectin from citrus peel wastes: A mechanistic study. *Food Hydrocolloids, 133*, Article 107778. https://doi.org/10.1016/J.FOODHYD.2022.107778
Huamani-Palomino, R. G., Pedro Ramos, M., Oliveira, G., Kock, F. V. C., Venâncio, T., & Córdova, B. M. (2023). Structural elucidation of pectin extracted from cocoa pod husk (Theobroma Cacao L.): Evaluation of the degree of esterification using FT-IR and 1H NMR. *Biomass Conversion and Biorefinery, 15*(2), 2047–2061. https://doi.org/10.1007/S13399-023-04082-3/METRICS
Iglesias, M. T., & Lozano, J. E. (2004). Extraction and characterization of sunflower pectin. *Journal of Food Engineering, 62*(3). https://doi.org/10.1016/S0260-8774(03)00234-6
Jarrín-Chacón, J. P., Núñez-Pérez, J., Espín-Valladares, R.d. C., Manosalvas-Quiroz, L. A., Rodríguez-Cabrera, H. M., & Pais-Chanfrau, J. M. (2023). Pectin extraction from residues of the cocoa fruit (*Theobroma cacao* L.) by different organic acids: A comparative study. *Foods, 12*(3), 590. https://doi.org/10.3390/FOODS12030590, 2023, Vol. 12, Page 590.
Jazayeri, S. M., Oviedo-Bayas, B., Guerrero-Chuez, R., Torres-Navarrete, Y., & Villamar-Torres, R. O. (2021). Environmental factors enhance production of plant secondary metabolites toward more tolerance and human health: Cocoa and coffee two model species. *Innovations in Biotechnology for a Sustainable Future*, 155–183. https://doi.org/10.1007/978-3-030-80108-3_9/TABLES/2
Jean-Marie, E., Jiang, W., Bereau, D., & Robinson, J. C. (2022). *Theobroma cacao* and *Theobroma grandiflorum*: Botany, composition and pharmacological activities of pods and seeds. *foods, 11*(24). https://doi.org/10.3390/foods11243966
Joint FAO/WHO Expert Committee on Food Additives. (2006). Combined compendium of food additive specifications. https://www.fao.org/4/a0691e/a0691e.pdf.
Kacuráková, M., Capek, P., Sasinková, V., Wellner, N., & Ebringerová, A. (2000). FT-IR study of plant cell wall model compounds: Pectic polysaccharides and hemicelluloses. *Carbohydrate Polymers, 43*(2), 195–203. https://doi.org/10.1016/S0144-8617(00)00151-X
Kazemi, M., Amiri Samani, S., Ezzati, S., Khodaiyan, F., Hosseini, S. S., & Jafari, M. (2021). High-quality pectin from cantaloupe waste: Eco-friendly extraction process, optimization, characterization and bioactivity measurements. *Journal of the Science of Food and Agriculture, 101*(15). https://doi.org/10.1002/jsfa.11327
Kieck, J. S., Zug, K. L. M., Huamaní Yupanqui, H. A., Gómez Aliaga, R., & Cierjacks, A. (2016). Plant diversity effects on crop yield, pathogen incidence, and secondary metabolism on cacao farms in Peruvian Amazonia. *Agriculture, Ecosystems and Environment, 222*. https://doi.org/10.1016/j.agee.2016.02.006
Konishi, T., Ono, H., Ohnishi-Kameyama, M., Kaneko, S., & Ishii, T. (2006). Identification of a mung bean arabinofuranosyltransferase that transfers arabinofuranosyl residues onto (1, 5)-linked α-l-arabino-oligosaccharides. *Plant Physiology, 141*(3), 1098–1105. https://doi.org/10.1104/PP.106.080309
Kontogianni, V. G., Charisiadis, P., Primikyri, A., Pappas, C. G., Exarchou, V., Tzakos, A. G., & Gerothanassis, I. P. (2013). Hydrogen bonding probes of phenol –OH groups. *Organic & Biomolecular Chemistry, 11*(6), 1013–1025. https://doi.org/10.1039/C2OB27117F
Li, W. J., Fan, Z. G., Wu, Y. Y., Jiang, Z. G., & Shi, R. C. (2019). Eco-friendly extraction and physicochemical properties of pectin from jackfruit peel waste with subcritical water. *Journal of the Science of Food and Agriculture, 99*(12), 5283–5292. https://doi.org/10.1002/JSFA.9729. WGROUP:STRING:PUBLICATION.
Liu, D., Xia, W., Liu, J., Wang, X., & Xue, J. (2024). Ultrasound-assisted alkali extraction of RG-I enriched pectin from thinned young apples: Structural characterization and gelling properties. *Food Hydrocolloids, 151*, Article 109879. https://doi.org/10.1016/J.FOODHYD.2024.109879
Macías-Garbett, R., Sosa-Hernández, J. E., Iqbal, H. M. N., Contreras-Esquivel, J. C., Chen, W. N., Melchor-Martínez, E. M., & Parra-Saldívar, R. (2022). Combined pulsed electric field and microwave-assisted extraction as a green method for the recovery of antioxidant compounds with electroactive potential from coffee agro-waste. *Plants, 11*(18). https://doi.org/10.3390/plants11182362
Mannino, G., Chinigò, G., Serio, G., Genova, T., Gentile, C., Munaron, L., & Bertea, C. M. (2021). Proanthocyanidins and where to find them: A meta-analytic approach to investigate their chemistry, biosynthesis, distribution and effect on human health. *antioxidants, 10*(8). https://doi.org/10.3390/antiox10081229
Manrique, G. D., & Lajolo, F. M. (2002). FT-IR spectroscopy as a tool for measuring degree of methyl esterification in pectins isolated from ripening papaya fruit. *Postharvest Biology and Technology, 25*(1). https://doi.org/10.1016/S0925-5214(01)00160-0
Mar, J. M., da Fonseca Júnior, E. Q., Corrêa, R. F., Campelo, P. H., Sanches, E. A., & Bezerra, J.d. A. (2024). *Theobroma* spp.: A review of it's chemical and innovation potential for the food industry. *Food chemistry Advances, 4*, Article 100683. https://doi.org/10.1016/J.FOCHA.2024.100683
Marasca, N., Brito, M. R., Rambo, M. C. D., Pedrazzi, C., Scapin, E., & Rambo, M. K. D. (2022). Analysis of the potential of cupuaçu husks (*Theobroma grandiflorum*) as raw material for the synthesis of bioproducts and energy generation. *Food Science and Technology, 42*, Article e48421. https://doi.org/10.1590/FST.48421
Marchiosi, R., dos Santos, W. D., Constantin, R. P., de Lima, R. B., Soares, A. R., Finger-Teixeira, A., … Ferrarese-Filho, O. (2020). Biosynthesis and metabolic actions of

simple phenolic acids in plants. *Phytochemistry Reviews, 19*(4), 865–906. https://doi.org/10.1007/S11101-020-09689-2, 2020 19:4.

Mellinas, A. C., Jiménez, A., & Garrigós, M. C. (2020). Optimization of microwave-assisted extraction of cocoa bean shell waste and evaluation of its antioxidant, physicochemical and functional properties. *LWT, 127*. https://doi.org/10.1016/j.lwt.2020.109361

Muñoz-Almagro, N., Molina-Tijeras, J. A., Montilla, A., Vezza, T., Sánchez-Milla, M., Rico-Rodríguez, F., & Villamiel, M. (2023). Pectin from sunflower by-products obtained by ultrasound: Chemical characterization and in vivo evaluation of properties in inflammatory bowel disease. *International Journal of Biological Macromolecules, 246*. https://doi.org/10.1016/j.ijbiomac.2023.125505

Munteanu, I. G., & Apetrei, C. (2021). Analytical methods used in determining antioxidant activity: A review. *International Journal of Molecular Sciences, 22*(7). https://doi.org/10.3390/ijms22073380

Munzert, K. S., & Engelsdorf, T. (2024). Plant cell wall structure and dynamics in plant–pathogen interactions and pathogen defence. *Journal of Experimental Botany*. , Article erae442. https://doi.org/10.1093/jxb/erae442

Nešić, A., Ružić, J., Gordić, M., Ostojić, S., Micić, D., & Onjia, A. (2017). Pectin-polyvinylpyrrolidone films: A sustainable approach to the development of biobased packaging materials. *Composites Part B: Engineering, 110*. https://doi.org/10.1016/j.compositesb.2016.11.016

Nisar, T., Wang, Z. C., Yang, X., Tian, Y., Iqbal, M., & Guo, Y. (2018). Characterization of citrus pectin films integrated with clove bud essential oil: Physical, thermal, barrier, antioxidant and antibacterial properties. *International Journal of Biological Macromolecules, 106*. https://doi.org/10.1016/j.ijbiomac.2017.08.068

Oñate-Gutiérrez, J. A., Díaz-Sánchez, L. M., Urbina, D. L., Pinzón, J. R., Blanco-Tirado, C., & Combariza, M. Y. (2023). Exploring the chemical composition and coloring qualities of cacao fruit epicarp extracts. *RSC Advances, 13*(19), 12712–12722. https://doi.org/10.1039/D3RA01049J

Pan, J., Li, C., Liu, J., Jiao, Z., Zhang, Q., Lv, Z., … Liu, H. (2024). Polysaccharide-based packaging coatings and films with phenolic compounds in preservation of fruits and vegetables—A review. *Foods, 13*(23), 3896. https://doi.org/10.3390/FOODS13233896, 2024, Vol. 13, Page 3896.

Patova, O. A., Luanda, A., Paderin, N. M., Popov, S. V., Makangara, J. J., Kuznetsov, S. P., & Kalmykova, E. N. (2021). Xylogalacturonan-enriched pectin from the fruit pulp of Adansonia digitata: Structural characterization and antidepressant-like effect. *Carbohydrate Polymers, 262*, Article 117946. https://doi.org/10.1016/J.CARBPOL.2021.117946

Peighambardoust, S. H., Jafarzadeh-Moghaddam, M., Pateiro, M., Lorenzo, J. M., & Domínguez, R. (2021). Physicochemical, thermal and rheological properties of pectin extracted from sugar beet pulp using subcritical water extraction process. *Molecules, 26*(5). https://doi.org/10.3390/molecules26051413

Peng, Y., & Wu, S. (2010). The structural and thermal characteristics of wheat straw hemicellulose. *Journal of Analytical and Applied Pyrolysis, 88*(2), 134–139. https://doi.org/10.1016/J.JAAP.2010.03.006

Pereira, P. H. F., Oliveira, T.Í. S., Rosa, M. F., Cavalcante, F. L., Moates, G. K., Wellner, N., … Azeredo, H. M. C. (2016). Pectin extraction from pomegranate peels with citric acid. *International Journal of Biological Macromolecules, 88*. https://doi.org/10.1016/j.ijbiomac.2016.03.074

Puchol-Miquel, M., Palomares, C., Fernández-Segovia, I., Barat, J. M., & Perez-Esteve, É. (2021). Effect of the type and degree of alkalization of cocoa powder on the physico-chemical and sensory properties of sponge cakes. *LWT, 152*. https://doi.org/10.1016/j.lwt.2021.112241

Qian, J., Zhao, F., Gao, J., Qu, L. J., He, Z., & Yi, S. (2021). Characterization of the structural and dynamic changes of cell wall obtained by ultrasound-water and ultrasound-alkali treatments. *Ultrasonics Sonochemistry, 77*, Article 105672. https://doi.org/10.1016/J.ULTSONCH.2021.105672

Reszczyńska, E., & Hanaka, A. (2020). Lipids composition in plant membranes. *Cell Biochemistry and Biophysics, 78*(4), 401. https://doi.org/10.1007/S12013-020-00947-W

Safirzadeh, S., Chorom, M., Karimi, R., Ariz, A., Behravan, H. R., & Fadami, M. (2017). Effects of alkaline pretreatments on chemical composition of sugarcane bagasse for easy degradation in soil. *Sugar Tech, 19*(1), 89–94. https://doi.org/10.1007/S12355-016-0435-0/FIGURES/3

Said, N. S., Olawuyi, I. F., & Lee, W. Y. (2023). Pectin hydrogels: Gel-forming behaviors, mechanisms, and food applications. *gels, 9*(9). https://doi.org/10.3390/gels9090732. Multidisciplinary digital publishing institute (MDPI).

Sanchez-Ballesta, M. T., Maoz, I., & Figueroa, C. R. (2022). Editorial: Secondary metabolism and fruit quality. *Frontiers in Plant Science, 13*. https://doi.org/10.3389/fpls.2022.1072193

Sandarani, M. (2017). A review: Different extraction techniques of pectin. *Journal of Pharmacognosy & Natural Products, 03*(03). https://doi.org/10.4172/2472-0992.1000143

Shi, H., Yu, L., Shi, Y., Lu, J., Teng, H., Zhou, Y., & Sun, L. (2017). Structural characterization of a rhamnogalacturonan I domain from ginseng and its inhibitory effect on galectin-3. *Molecules, 22*(6), 1016. https://doi.org/10.3390/MOLECULES22061016, 2017, Vol. 22, Page 1016.

Siqueira, R. A., Veras, J. M. L., de Sousa, T. L., de Farias, P. M., de Oliveira Filho, J. G., Bertolo, M. R. V., … Plácido, G. R. (2022). Pequi mesocarp: A new source of pectin to produce biodegradable film for application as food packaging. *Food Science and Technology, 42*. https://doi.org/10.1590/fst.71421

Slimestad, R., Holm, V., & Barsett, H. (2019). Sample preparation and analysis of tomato pectin monomers. *Chromatographia, 82*(6). https://doi.org/10.1007/s10337-019-03719-8

Sun, B., Ricardo-da-Silva, J. M., & Spranger, I. (1998). Critical factors of vanillin assay for catechins and proanthocyanidins. *Journal of Agricultural and Food Chemistry, 46*(10). https://doi.org/10.1021/jf980366j

Tauchen, J., Bortl, L., Huml, L., Miksatkova, P., Doskocil, I., Marsik, P., … Kokoska, L. (2016). Phenolic composition, antioxidant and anti-proliferative activities of edible and medicinal plants from the Peruvian Amazon. *Revista Brasileira de Farmacognosia, 26*(6), 728–737. https://doi.org/10.1016/J.BJP.2016.03.016

Valverde, D., Behrends, B., Pérez-Esteve, Kuhnert, N., & Barat, J. M. (2020). Functional changes induced by extrusion during cocoa alkalization. *Food Research International, 136*. https://doi.org/10.1016/j.foodres.2020.109469

van Vliet, J. A., & Giller, K. E. (2017). Mineral nutrition of cocoa: A review. *Advances in Agronomy, 141*. https://doi.org/10.1016/bs.agron.2016.10.017

Vázquez-Ovando, A., Molina-Freaner, F., Nuñez-Farfán, J., Betancur-Ancona, D., & Salvador-Figueroa, M. (2015). Classification of cacao beans (Theobroma cacao L.) of southern Mexico based on chemometric analysis with multivariate approach. *European Food Research and Technology, 240*(6). https://doi.org/10.1007/s00217-015-2415-0

Vincken, J. P., Schols, H. A., Oomen, R. J. F. J., McCann, M. C., Ulvskov, P., Voragen, A. G. J., & Visser, R. G. F. (2003). If homogalacturonan were a side chain of rhamnogalacturonan I. Implications for cell wall architecture. *Plant Physiology, 132*(4), 1781–1789. https://doi.org/10.1104/PP.103.022350

Vriesmann, L. C., Teófilo, R. F., de Oliveira, L., & Petkowicz, C. (2012). Extraction and characterization of pectin from cacao pod husks (Theobroma cacao L.) with citric acid. *LWT, 49*(1), 108–116. https://doi.org/10.1016/J.LWT.2012.04.018

Walther, D. J., Peter, J. U., Bashammakh, S., Hörtnagl, H., Voits, M., Fink, H., & Bader, M. (2003). Synthesis of serotonin by a second tryptophan hydroxylase isoform. *Science, 299*(5603), 76. https://doi.org/10.1126/SCIENCE.1078197

Wang, W., Ma, X., Jiang, P., Hu, L., Zhi, Z., Chen, J., Ding, T., Ye, X., & Liu, D. (2016). Characterization of pectin from grapefruit peel: A comparison of ultrasound-assisted and conventional heating extractions. *Food Hydrocolloids, 61*, 730–739. https://doi.org/10.1016/J.FOODHYD.2016.06.019

Waterman, P. G., & Mole, S. (1994). *Analysis of phenolic plant metabolites* (1st ed.) (1st ed., Vol. 83). Wiley-Blackwell.

Werner, K., Pommer, L., & Broström, M. (2014). Thermal decomposition of hemicelluloses. *Journal of Analytical and Applied Pyrolysis, 110*(1), 130–137. https://doi.org/10.1016/J.JAAP.2014.08.013

Wu, J., Shen, S., Gao, Q., Yu, C., Cheng, H., Pan, H., … Chen, J. (2023a). RG-I domain matters to the in vitro fermentation characteristics of pectic polysaccharides recycled from Citrus canning processing water. *Foods, 12*(5), 943. https://doi.org/10.3390/FOODS12050943, 2023, Vol. 12, Page 943.

Wu, J., Shen, S., Gao, Q., Yu, C., Cheng, H., Pan, H., … Chen, J. (2023b). RG-I domain matters to the in vitro fermentation characteristics of pectic polysaccharides recycled from citrus canning processing water. *Foods, 12*(5). https://doi.org/10.3390/FOODS12050943

Yang, Z., Zhang, Y., Jin, G., Lei, D., & Liu, Y. (2024). Insights into the impact of modification methods on the structural characteristics and health functions of pectin: A comprehensive review. *International Journal of Biological Macromolecules, 261*, Article 129851. https://doi.org/10.1016/J.IJBIOMAC.2024.129851

Zhang, C., Slegers, P. M., Wisse, J., Sanders, J. P. M., & Bruins, M. E. (2018). Sustainable scenarios for alkaline protein extraction from leafy biomass using green tea residue as a model material. *Biofuels, Bioproducts and Biorefining, 12*(4), 586–599. https://doi.org/10.1002/BBB.1870